CHAPTER 7

COMPOSITIONS OF ISOMETRIES

7.0   Isometry 'hunting'

7.0.1 <u>Nothing totally new.</u> Already in 4.0.4 we saw that the composition (combined effect) of a rotation followed by a translation is another rotation, by the same angle but about a different center. And we employed this fact (in the special case of 180^0 rotation) in 6.5.3 (**'visual proof'** in figure 6.44) in our study of two-colored **p2** patterns. In fact we did run into several compositions of isometries in chapter 6: for example, figure 6.54 demonstrated that the composition of two perpendicular glide reflections is a 180^0 rotation; and we encountered instances of composition of two rotations in figures 6.44, 6.99, and 6.128.

Speaking of glide reflection, recall that its definition (1.4.2) involves the **commuting** composition of a reflection and a translation parallel to it. Moreover, we also pointed out in 1.4.2 that, in the composition of a reflection and a translation non-parallel to each other, whatever isometry that might be, the **order** of the two isometries does matter (figure 1.32). And we did indicate in figure 6.13 that the composition of a glide reflection (hence reflection as well) followed by a translation is a new glide reflection (about an axis parallel to the original and by a vector of different length).

7.0.2 <u>'No way out'.</u> Of course the most important point made in 1.4.2, if not in the entire book, is that the composition $I_2 * I_1$ of every two isometries I_1, I_2 **must** again be an isometry: indeed the distance between every two points P, Q is equal, because I_1 is an isometry, to the distance between $I_1(P)$ and $I_1(Q)$; which is in turn equal, because I_2 is an isometry, to the distance between $I_2(I_1(P)) = I_2 * I_1(P)$ and

$I_2(I_1(Q)) = I_2*I_1(Q)$. In particular, the composition of every two isometries of a wallpaper pattern must be an isometry of it: this turns its set of isometries into a **group**. (More on this in chapter 8!)

So we do know that the composition I_2*I_1 of any two given isometries I_1, I_2 is again an isometry. Since (section 1.5) there exist **only four** possibilities for planar isometries (translation, rotation, reflection, glide reflection), determining I_2*I_1 should in principle be relatively simple. On the other hand, our remarks in 7.0.1 and overall experience so far indicate that there may after all be certain practical difficulties: formulas like the ones employed in chapter 1 may be too complicated for the mathematically naive (and not only!), while visual 'proofs' like the ones you saw throughout chapter 6 are not rigorous enough for the mathematician at heart. Therefore we prefer to base our conclusions in this chapter (and study of the **ten** possible combinations of isometries) on solid **geometrical proofs**: those are going to be as precise as algebraic proofs are, relying on the directness of pictures at the same time.

7.0.3 <u>A 'painted' bathroom wall.</u> Before we provide a detailed study of all possible combinations of isometries (sections 7.1-7.10), we present below a more **'empirical'** approach. Employing a 'standard' coloring of the familiar bathroom wall we seek to 'guess' -- **'hunt'** for, if you like -- the composition **T∗R$_0$** (clockwise 90^0 rotation followed by diagonal SW-NE translation, see figure 7.1) already determined in 4.0.4, dealing with other issues on the way. (The coordinate system of figure 4.3 is absent from figure 7.1, and the lettering/numbering of the tiles has given way to coloring.)

So, why the colors? First of all they help us, thanks to the **maplike** coloring, distinguish between neighboring tiles and keep track of where each tile is mapped under the various isometries of the tiling (and their compositions). Moreover, since the coloring is **consistent**, if the composition in question sends, say, **one** red tile to a green tile, then we know that it must send **every** red tile to some green tile: that helps us 'remember' (and even decide) where specific tiles are mapped by the 'unknown' isometry-composition (of the two isometries that we need to determine) without having to

'keep notes' on them. (All this assumes that you will take the time to color the tiles as suggested in figure 7.1, of course; but you do not have to, as long as you can keep track of where your tiles go!)

Most important, the colored tiles will help you rule out many possibilities. To elaborate, let's first look at **T∗R₀**'s **color effect**:

R_0	T	$T*R_0$
B → R	R → G	B → G
Y → G	G → R	Y → R
R → Y	Y → B	R → B
G → B	B → Y	G → Y

In other words, all we did was to rewrite **T∗R₀** (in the language of color **permutations**) as **(RG)(BY)∗(BRYG) = (BGYR)**. Now there exist many isometries whose effect on color is **(BGYR)**, such as the four 90^0 rotations around the red (**R**) square -- two of them (**R₁**, **R₂**) counterclockwise and two of them clockwise -- and the four diagonal glide reflections in figure 7.1: which one of these isometries, **if any**, is **T∗R₀**?

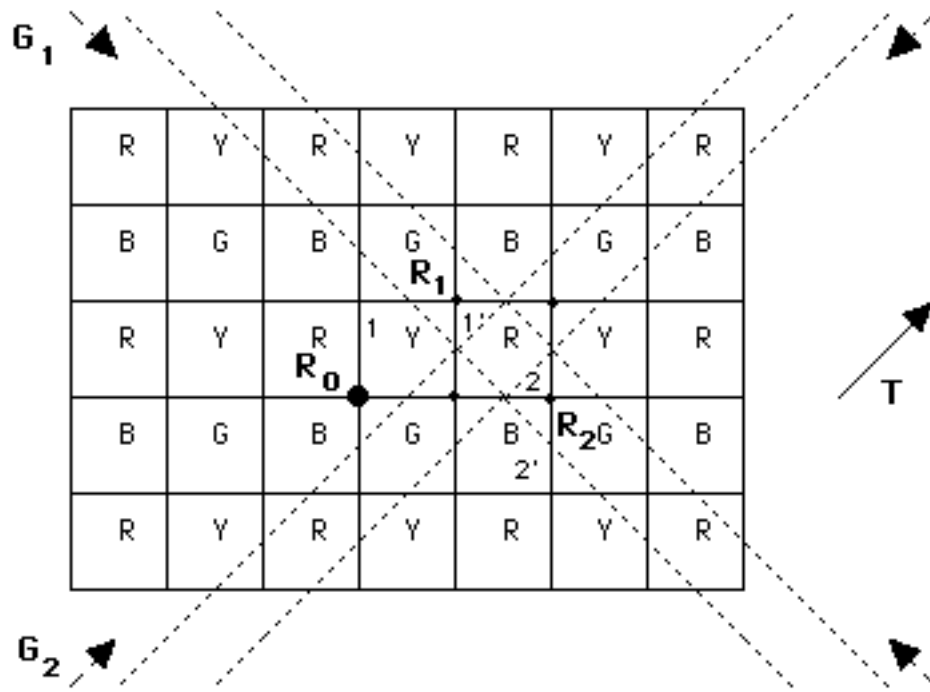

Fig. 7.1

Well, before we decide what $T*R_0$ is, let's quickly observe what it **cannot** possibly be: since all translations, reflections, vertical or horizontal glide reflections, 180^0 rotations, and 90^0 rotations of first kind (i.e., centered in the middle of a tile) produce a color effect equal to either a product of two 2-cycles or a 2-cycle or the identity **P** (instead of a 4-cycle like **(BGYR)**), none of these isometries could possibly be $T*R_0$. (For some examples, notice that the vertical reflection passing through R_0 is **(BG)(YR)**, the left-to-right glide reflections passing through R_0 are either **(BY)(GR)** or **(BR)(GY)**, minimal vertical translation is **(BR)(GY)**, 90^0 rotation about the center of any red or green square is **(BY)**, vertical or horizontal reflections passing through such centers are **P**, etc.) So, the only possibilities left are the ones that figure 7.1 'suggests'.

Now many students would naturally look at the outcome that we ruled out in 4.0.4, that is R_1. To be more precise, at 4.0.4 we looked at **clockwise** 90^0 rotation at R_1 (the translation of clockwise 90^0 R_0 by **T**), which we can now rule out at once: its color effect is **(BRYG)**, not $T*R_0$'s **(BGYR)**. But how about **counterclockwise** 90^0 rotation at R_1, whose color effect is **(BGYR)**, after all? Well, looking (figure 7.1) at the yellow tile labeled #1, we see that R_0 takes it to the green tile directly south of it, which is in turn mapped by **T** to the red tile labeled #1′ (figure 7.1); that's exactly where counterclockwise R_1 moves tile #1, so it is **tempting** to guess that it equals $T*R_0$: after all, the two isometries **seem** to agree not only in terms of color, but **position**, too! Well, the temptation should be resisted: for example, $T*R_0$ moves the red tile #2 (formerly #1′) to the blue tile #2′ (by way of the yellow tile at the bottom center of figure 7.1), but counterclockwise R_1 maps #2 to the blue tile directly north of it: if two isometries disagree on a single tile they simply cannot be one and the same.

So, are there any other 'good candidates' out there? Notice that counterclockwise R_2 agrees with $T*R_0$ on #2, but not #1, while G_2 agrees with $T*R_0$ on #1, but not #2. More promising is G_1, which agrees with $T*R_0$ on **both** #1 and #2: shouldn't the agreement on

two tiles allow us to conclude that these two isometries are equal? Well, at this point you need to go back to 3.3.4, where we discussed how and why "every isometry on the plane is uniquely determined by its effect on **any three non-collinear points**": replace points by **tiles**, and surely you will begin to suspect that G_1 may not be the right answer after all; indeed this is demonstrated in figure 7.2, where we see that the blue tile #3 is mapped to a green tile #3′ by $T*R_0$ but to a green tile #3″ by G_1.
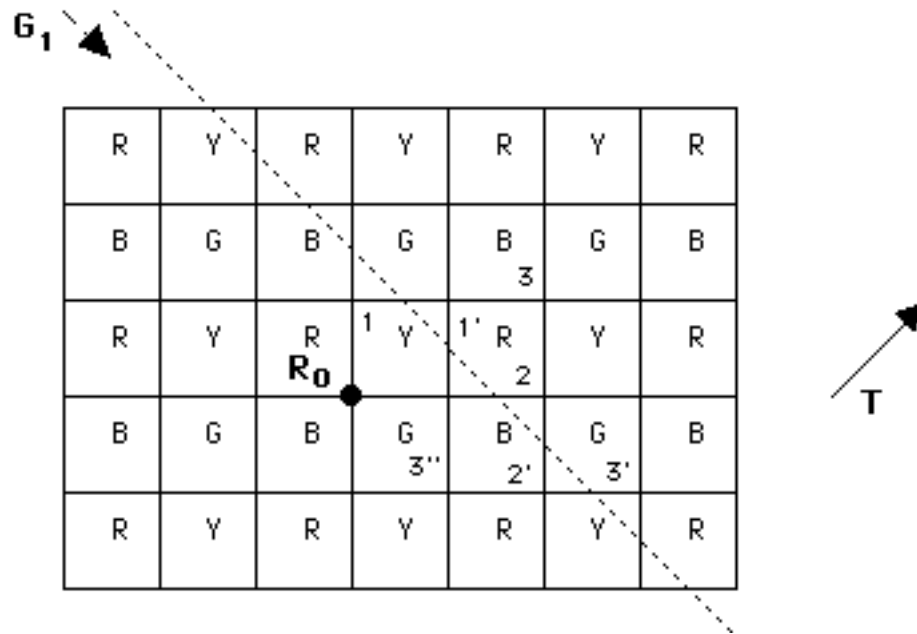
Fig. 7.2

Now a closer look at figure 7.2 reveals that G_1, and, more generally, any glide reflection, had no chance at all: indeed, looking at the tile trio **123** and its image **1′2′3′**, we see that they are **homostrophic**, hence only a rotation could possibly work! But we have already tried a couple of rotations and none of them worked! Well, if you are about to give up on trial-and-error, if you feel lost in this forest of tiles and possibilities, chapter 3 comes to your rescue again: simply determine the center of a rotation that maps the **centers** of tiles #1, #2, #3 to the centers of the tiles #1′, #2′, #3′; this is in fact done in figure 7.3, where the rotation center is determined as the intersection of the three **perpendicular bisectors** 11′, 22′, and 33′. (Of course **just two** perpendicular bisectors would suffice, as we have seen in 3.3.5).
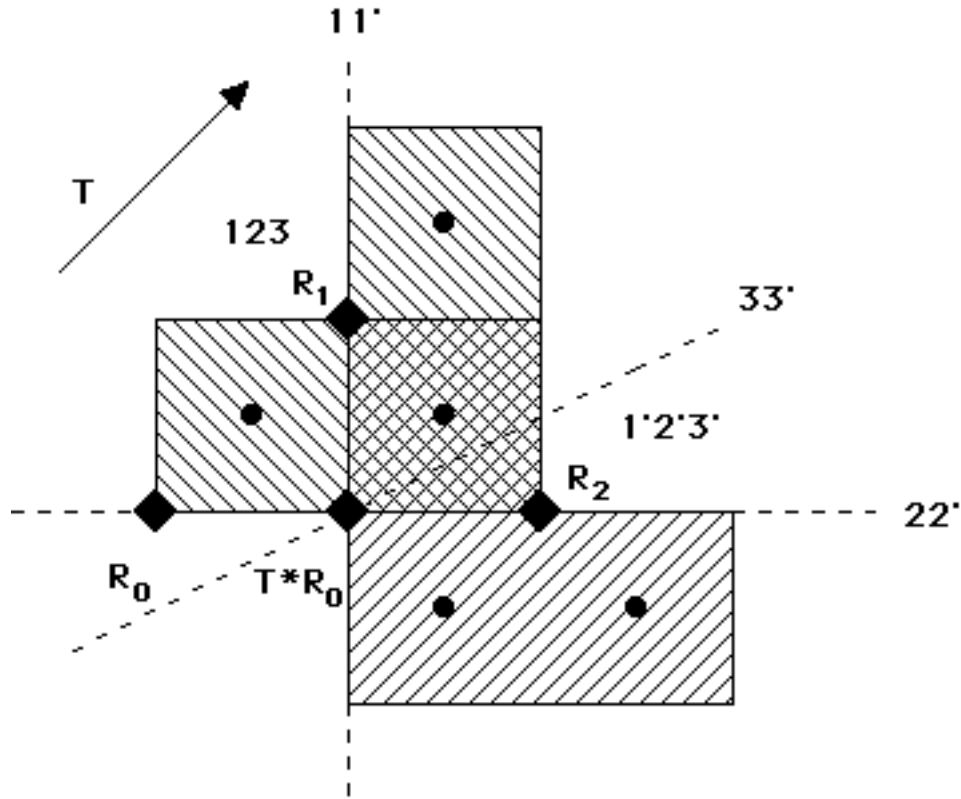
Fig. 7.3

So, it becomes clear after all that a clockwise 90^0 rotation maps the tile trio **123** (NW-SE shading) to the tile trio **1′2′3′** (NE-SW shading); that rotation **has** to be **T∗R$_0$**, and its center is located 'between' the three centers **R$_0$**, **R$_1$**, and **R$_2$** (all indicated by a black square in figure 7.3). We could very well have made the right guess earlier, but the chapter 3 method illustrated in figure 7.3 can **always** be applied after the first few guesses have failed! (An extra advantage is the replacement of **D$_4$** sets (squares) by **D$_1$** sets (trios of non-collinear squares), which facilitates isometry recovery.)

7.0.4 <u>Additional examples.</u> In figure 7.4 we demonstrate the determination of **R$_0$∗G$_1$** and **G$_1$∗R$_0$**, where **R$_0$** is again a 90^0 clockwise rotation. In the case of **R$_0$∗G$_1$**, the color effect is just the identity **P = (BRYG)∗(BGYR)**: the details are as in 7.0.3 above. That immediately rules out all the rotations (save for one type of 180^0 rotation revealed towards the end of this section) and **'off-tile-center'** reflections: none of those isometries, in the case of the

particular tiling and coloring, always, may preserve all the colors; less obviously, the same is true of **diagonal** glide reflections. What could it be, then? Working again with individual tiles #1, #2, and #3 (figure 7.4), we see them mapped by R_0*G_1 to the tiles #1′, #2′, and #3′: the two tile trios **123** and **1′2′3′** are **heterostrophic**, hence the outcome must be a **'hidden'** glide reflection -- one of those glide reflections, first mentioned in 6.3.1, employing one of the tiling's **reflection axes** and one of the tiling's **translation vectors**. Either by applying the procedures of chapter 3 -- as in figure 7.3, but using midpoints instead of bisectors -- or by simple inspection, we find out that R_0*G_1 is indeed the hidden **vertical** glide reflection denoted in figure 7.4 by **MG′**: the importance of hidden glide reflections warrants the use of a separate notation!
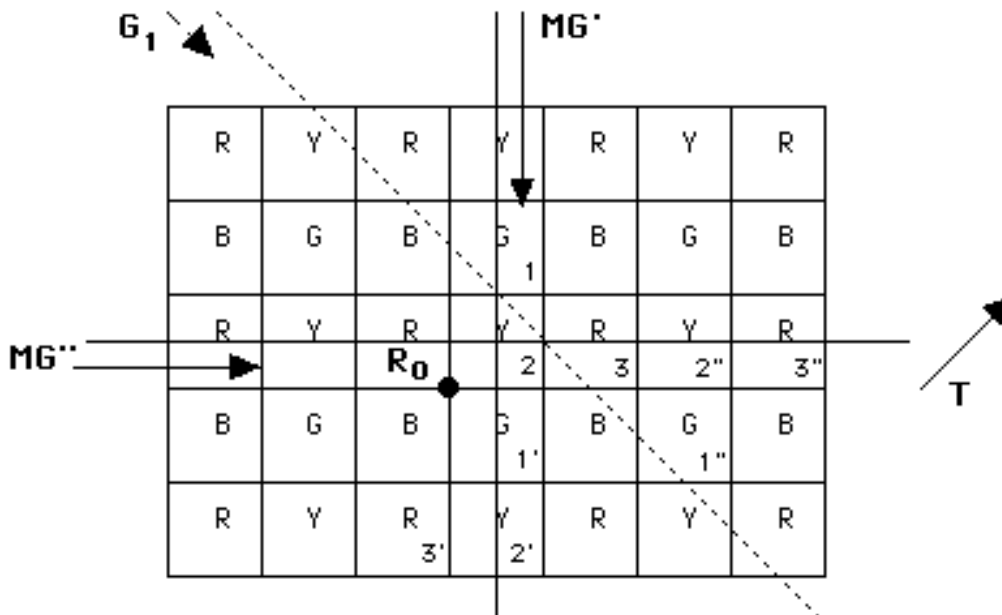
Fig. 7.4

    A similar analysis, employing the tile trios **123** and **1″2″3″**, shows G_1*R_0 to be **MG″**, a **horizontal** hidden glide reflection (figure 7.4): rather predictably, R_0*G_1 and G_1*R_0 are differently positioned isometries of exactly the same kind. Notice the importance, in each case, of having used three non-collinear tiles: had we used only tiles #1 and #2 for R_0*G_1, or #2 and #3 for G_1*R_0, we would have 'concluded' that those glide reflections were mere translations!

    Having seen the importance of order (of the two isometries) in

combining isometries, we turn now to the relevance of **angle orientation**: we investigate, in figure 7.5, the compositions $R_3^+*G_1$ and $R_3^-*G_1$, where R_3^- and R_3^+ are counterclockwise and clockwise 90^0 rotations about the shown center R_3, respectively.
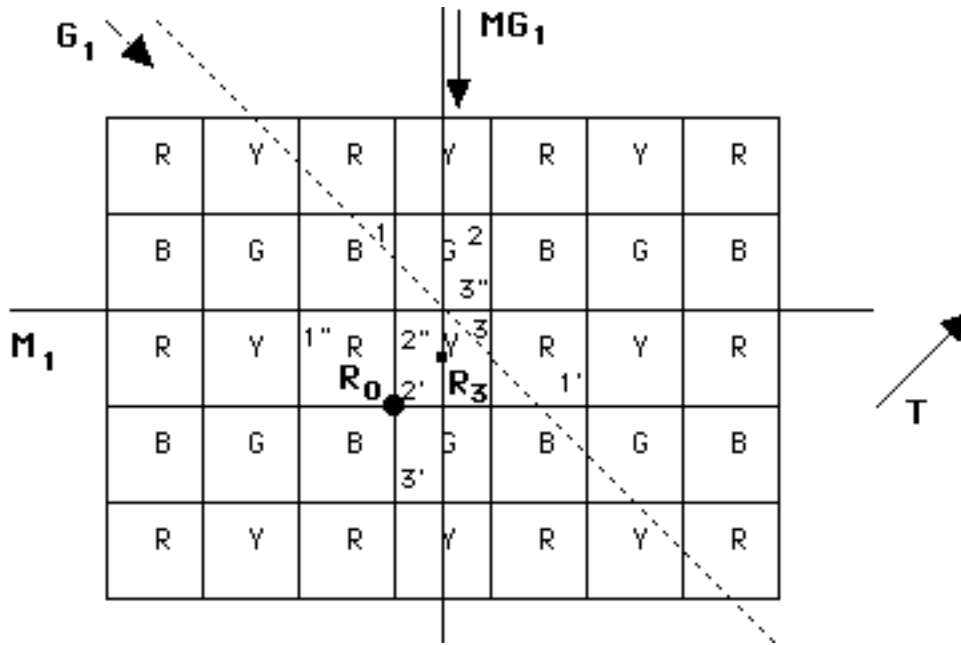

Fig. 7.5

Bypassing color considerations, but still using our 'tile trios' (**1′2′3′** for $R_3^+*G_1$, **1″2″3″** for $R_3^-*G_1$), let's look at the outcomes in figure 7.5. $R_3^+*G_1$ is a hidden glide reflection (MG_1) sharing the same axis with $MG' = R_0*G_1$ (figure 7.4), but of smaller (half) gliding vector: yes, the **distance** from the rotation center to the glide reflection axis does play a crucial role! And $R_3^-*G_1$ is a horizontal **reflection** (M_1): as R_3^- 'turns opposite' of G_1's gliding vector, it ends up annihilating it -- while R_3^+, 'turning the same way' as G_1's gliding vector, increases its length to that of MG_1's gliding vector!

How about compositions of glide reflections? Viewing, once again, a reflection as a glide reflection of zero gliding vector (1.4.8), we may first think of compositions like M_1*MG_1 and MG_1*M_1: those are rather easy in view of the discussion on perpendicular glide reflections in 6.6.2. For example, adjusting figure 6.54 to the

present circumstances, we see that $M_1 * MG_1$ is the 180^0 rotation centered at the green tile right above R_3, and this is corroborated by color permutations: $(BR)(GY)*(BR)(GY) = P$. (Recall (4.0.3) that every fourfold center may also act as a twofold center, in this case preserving all colors!) Turning now to $M_1 * G_1$ (figure 7.6), **probably** a rotation in view of 6.6.2, we see that its color effect is $(BR)(GY)*(BGYR) = (BY)$. The only **rotations** producing this color effect are 90^0 rotations centered **inside** a **green or red** tile (rather than at the common corner of four neighboring tiles); but there exist **many** such rotations, so it is best to once again resort to **position** considerations and numbered tiles!
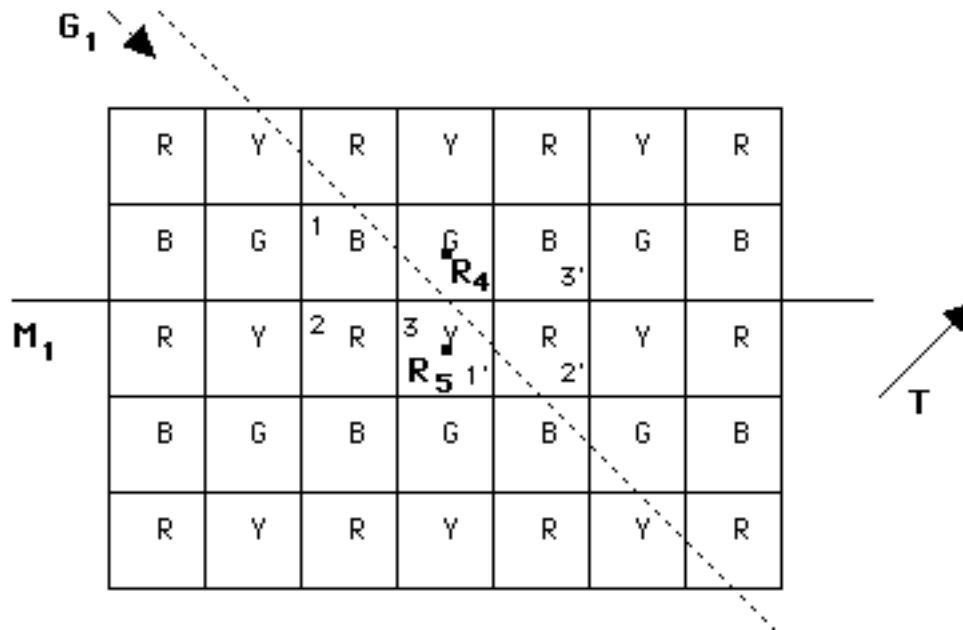
Fig. 7.6

Using three non-collinear tiles #1, #2, #3 (figure 7.6), we see that $M_1 * G_1$ maps the tile trio **123** to **1′2′3′**: these two trios are **homostrophic**, corroborating our guess that $M_1 * G_1$ is a rotation. And since we already know, through our **color** considerations above, that the composition in question must be a 90^0 rotation centered inside a green or red tile, the answer becomes obvious: $M_1 * G_1$ is the shown 90^0 **counterclockwise** rotation centered at R_4. Work along similar lines will allow you to show that $G_1 * M_1$ is the **clockwise** 90^0 rotation R_5 (of color effect $(GR) = (BGYR)*(BR)(GY)$).

We could go on, looking not only at more combinations but at different colorings and types of tilings as well, but we would rather start looking at composition of isometries in a more systematic manner, just as promised in 7.0.2.

7.1   Translation ∗   Translation

7.1.1 <u>Just the parallelogram rule.</u> Composing two translations T_1, T_2, each of them represented by a vector, is like computing the combined effect of two forces (vectors) in high school Physics: all we need is the **parallelogram rule** as shown in figure 7.7 (and applied to a particular point P, where each of the two vectors has been applied).
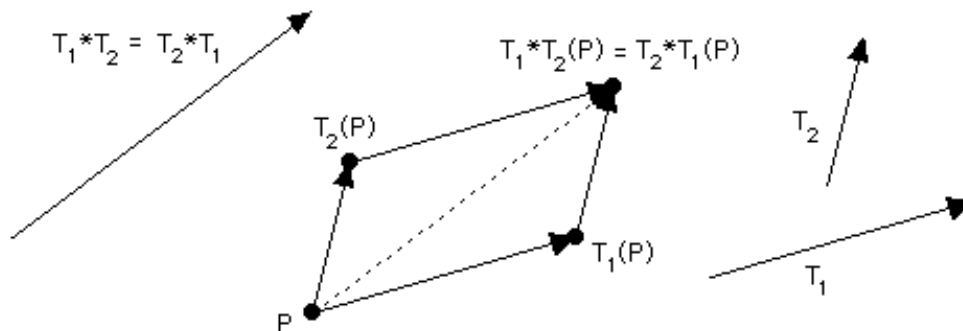
Fig 7.7

The composition is simply represented by the **'diagonal'** vector, and the equality $T_1*T_2 = T_2*T_1$ is another way of saying that there are **two ways** of 'walking' (across the parallelogram's edges) from P to the diagonal's other end (figure 7.7). So, every two translations **commute** with each other, something that happens only in a few cases of other isometries (such as the composition of reflection and translation parallel to each other discussed in 1.4.2 and 7.0.1).

7.1.2 <u>Collinear translations.</u> When the translation vectors are collinear (parallel) to each other (as in the **border patterns** of chapters 2 and 5, for example), then the Physics becomes easier and

the parallelogram of figure 7.7 is **flattened**. In fact, every two parallel vectors T_1, T_2 of lengths l_1, l_2 may be written as $\pm l_1 \times T$, $\pm l_2 \times T$, where **T** is a vector of length 1; the choice between + or − depends on whether or not **T** and the vector in question (T_1 or T_2) are of the same or opposite orientation (**sense**), respectively. The composition of the two translations is then reduced to addition of real numbers by way of $T_2 * T_1 = (\pm l_1 \pm l_2) \times T$. Conversely, given any vector **T**, not necessarily of length 1, all vectors parallel to it are of the form $l \times T$, where l may be any positive or negative real number.

Combining 7.1.1 and 7.1.2, we may now talk about **linear combinations** of non-collinear translations T_1, T_2: those are sums of the form $l_1 \times T_1 + l_2 \times T_2$, where l_1, l_2 are any real numbers ... and have already been employed in figures 4.10 & 4.11 (where we had in fact indicated, without saying so, that every translation in a wallpaper pattern may be written as a linear combination (with l_1, l_2 **integers**) of two particular translations).

7.2   Reflection ∗ Reflection

7.2.1 <u>Parallel axes (translation).</u> Back in 2.2.3, we did observe that the distance between every two **adjacent** mirrors in a **pm11** pattern is equal to **half** the length of the pattern's **minimal** translation vector. This makes full sense in view of the following 'proof without words':
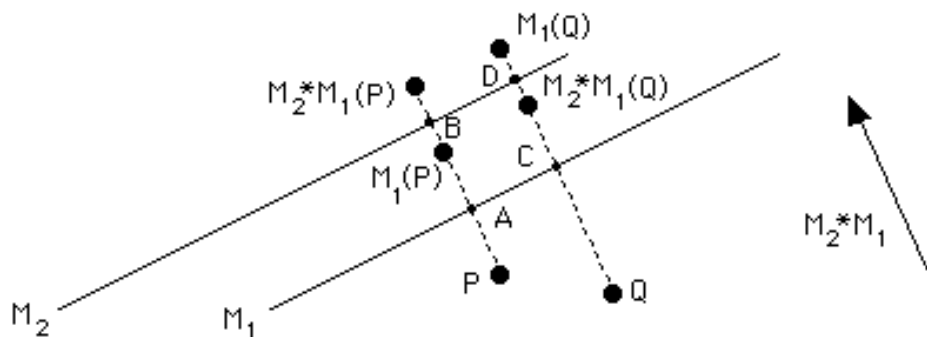

Fig. 7.8

Well, we can add a few words after all: with **d(X, Y)** standing for **distance** between points X and Y, we see that d(P, M_2*M_1(P)) = d(P, M_1(P)) + d(M_1(P), M_2*M_1(P)) = 2 × d(A, M_1(P)) + 2 × d(M_1(P), B) = 2 × d(A, B) = twice the distance between the parallel lines M_1 and M_2; likewise, d(Q, M_2*M_1(Q)) = d(Q, M_1(Q)) − d(M_1(Q), M_2*M_1(Q)) = 2 × d(C, M_1(Q)) − 2 × d(M_1(Q), D) = 2 × d(C, D) = twice the distance between the parallel lines M_1 and M_2. So, both P and Q moved in the same direction (**perpendicular** to M_1 and M_2, and **'from M_1 toward M_2'**) and by the same length (**twice** the distance between M_1 and M_2). We leave it to you to verify that the same will happen to any other point, regardless of its location (between the two reflection lines, 'north' of M_2, 'way south' of M_1, etc): always, the combined effect of M_1 and M_2 (in that **order**) is the **translation** vector M_2*M_1 shown in figure 7.8!

7.2.2 <u>Non-parallel axes.</u> We have not kept it a secret that the composition -- in this case **intersection** -- of two perpendicular reflections yields a half turn: we have seen this in 2.7.1 (**pmm2**), 4.6.1 (**pmm**), 4.9.1 (**cmm**), etc. Moreover, we have seen 120^0 centers (**p3m1**, **p31m**) at the intersections of three reflection axes (making angles of **60^0**), 90^0 centers (**p4m**) at the intersections of four reflection axes (making angles of **45^0**), and 60^0 centers (**p6m**) at the intersections of six reflection axes (making angles of **30^0**). It is therefore reasonable to conjecture that every two reflection axes intersecting each other at an angle $\phi/2$ generate a rotation about their intersection point by an angle ϕ; this is corroborated right below:
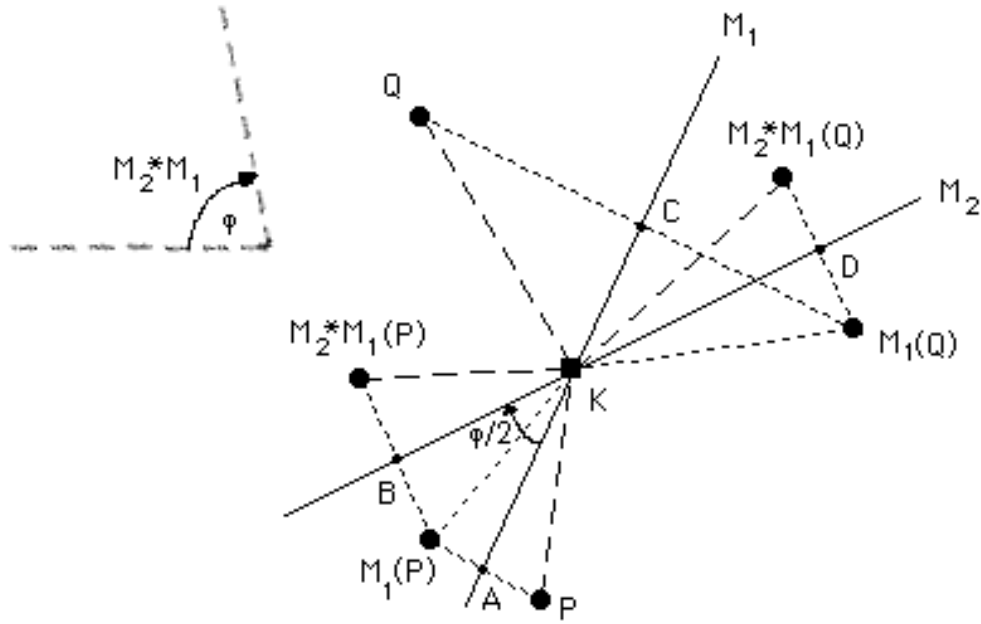
Fig. 7.9

To turn figure 7.9 into a proof, we must show, with **a(X, Y)** denoting the **angle** between lines KX and KY, that a(P, M_2*M_1(P)) = 2 × a(A, B), a(Q, M_2*M_1(Q)) = 2 × a(C, D), and so on. These equalities are derived **exactly** as the corresponding ones in 7.2.1, simply replacing **d** (distances) by **a** (angles). We leave it to you to verify that, no matter where P or Q is, the composition M_2*M_1 is a rotation by the angle shown in figure 7.9: **twice** the size of the **acute** angle between M_1 and M_2, and going '**from M_1 toward M_2**' (which happens to be clockwise in this case).

7.2.3 <u>The crucial role of reflections.</u> Unlike translations, reflections do **not** commute with each other: it is easy to see that M_1*M_2 is a vector opposite of M_2*M_1 in 7.2.1, while M_1*M_2 is an angle opposite (counterclockwise) of M_2*M_1 in 7.2.2. A crucial **exception** occurs when M_1 and M_2 are perpendicular to each other: there is no difference between a clockwise 180^0 rotation and a counterclockwise 180^0 rotation sharing the same center (1.3.10)!

All the techniques and observations of this section, including that of the preceding paragraph, stress the closeness between

translation and **rotation**: each of them may be represented as the composition of **two** reflections, and the outcome depends only on whether the angle between them is zero (translation) or non-zero (reflection). It follows at once that every **glide reflection** may be written as the composition of **three** reflections. So we may safely say, knowing that there exist no other planar isometries (section 1.5), that every isometry of the plane is the composition of **at most three reflections**.

Conversely, the **traditional way** of proving that there exist only four types of planar isometries is to show **first** that every isometry of the plane **must** be the composition of at most three reflections: see for example **Washburn & Crowe**, Appendix I. We certainly provided a classification of planar isometries not relying on this fact in section 1.5; but we will be analysing a translation or rotation into two reflections throughout chapter 7.

As a concluding remark, let us point out another difference between translation and rotation (and the way each of them may be written as a composition M_2*M_1 of reflections): in the case of a translation, we may vary the position of the parallel mirrors M_1, M_2 but not their distance or common direction; in the case of a rotation, we may vary the directions of M_1, M_2, but not their angle or intersection point.

7.3   Translation ∗ Reflection

7.3.1 <u>Perpendicular instead of parallel.</u> Of course we have already seen a most important special case of this combination in 1.4.2: when the translation and the reflection are parallel to each other, their **commuting** composition is useful and powerful enough to be viewed as an isometry of its own (glide reflection). Another important special case is the one that involves a translation and a reflection that are perpendicular to each other. We have encountered many such cases, the last one provided by 7.2.1: just think of the reflection M_1 followed by the translation M_2*M_1, yielding the equality $(M_2*M_1)*M_1 = M_2*(M_1*M_1) = M_2*I = M_2$; or of the translation

M_2*M_1 followed by the reflection M_2, leading to the equality $M_2*(M_2*M_1) = (M_2*M_2)*M_1 = I*M_1 = M_1$.

Our 'algebraic experimentation' (and appeal to 7.2.1) above suggests that the composition of a reflection **M** and a translation **T** perpendicular to each other is another reflection **parallel** to the original one; this is established below, via another appeal to 7.2.1:
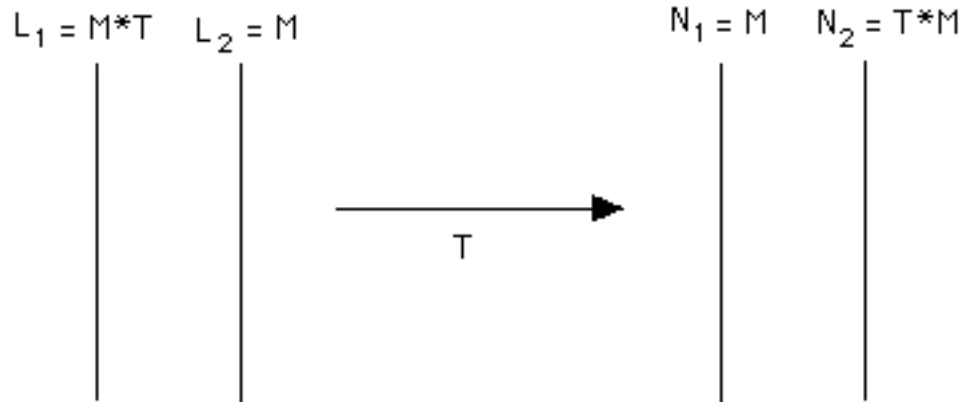
$$L_1 = M*T \quad L_2 = M \qquad\qquad N_1 = M \quad N_2 = T*M$$

T

Fig. 7.10

What went on in figure 7.10? We computed **both** compositions **M∗T** (left) and **T∗M** (right), writing **T** as a composition of two reflections perpendicular to it (therefore **parallel** to **M**) and at a distance from each other equal to half the length of **T** (7.2.1): in the first case, with **T**'s **second** reflection L_2 being **M**, **M∗T** equals $L_2*(L_2*L_1) = L_1$; and in the second case, with **T**'s **first** reflection N_1 being **M**, **T∗M** equals $(N_2*N_1)*N_1 = N_2$. (As above, it is crucial that the square of a reflection is the identity isometry **I**.)

So, we see that a reflection **M** and a translation **T** perpendicular to each other do not commute: when **T** comes first it moves **M** **'backward'** by |**T**|/2 (figure 7.10, left), and when **T** follows **M** it moves it **'forward'** by |**T**|/2 (figure 7.10, right); that is, **M∗T** and **T∗M** are **mirror images** of each other about **M**. You should try to verify these results, following the method, rather than the outcome, of 7.2.1 and figure 7.8.

7.3.2 Physics again! We come now to the general case of the

composition of a reflection **M** and a translation **T**, assuming **M** and **T** to be neither parallel nor perpendicular to each other: it looks complicated, but an old trick from high school Physics is all that is needed! Indeed, **analysing T** into two components, $\mathbf{T_1}$ (perpendicular to **M**) and $\mathbf{T_2}$ (parallel to **M**), we reduce the problem to known special cases; in figure 7.11 you see how $\mathbf{M*T} = \mathbf{M*(T_1*T_2)} = \mathbf{(M*T_1)*T_2} = \mathbf{M'*T_2}$ turns into a **glide reflection** (of axis $\mathbf{M*T_1}$ (at a distance of $|\mathbf{T_1}|/2$ from **M**) and vector $\mathbf{T_2}$):
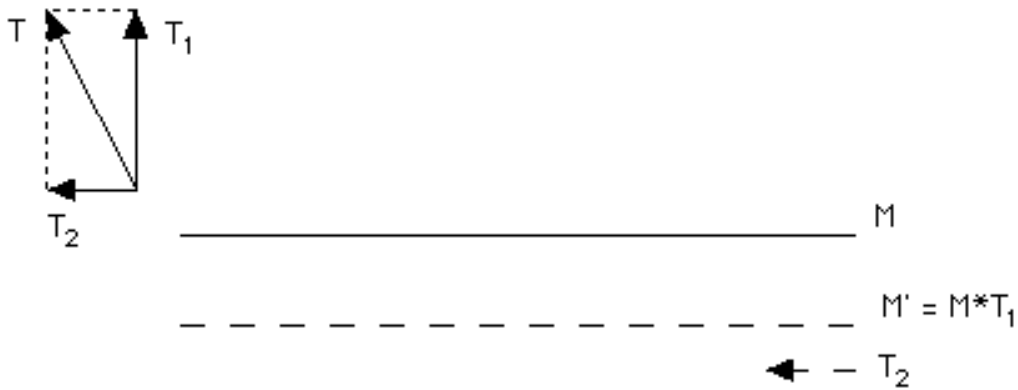
Fig. 7.11

Likewise, $\mathbf{T*M} = \mathbf{(T_2*T_1)*M} = \mathbf{T_2*(T_1*M)} = \mathbf{T_2*M''}$ is a glide reflection (not shown in figure 7.11) of vector $\mathbf{T_2}$ (no change here) and axis **M″** (mirror image of **M′** about **M**, as in 7.3.1). So, in general, the composition of a reflection **M** and a translation **T** is a glide reflection; and a closer look at this section's work shows that it is a reflection if and only if **M** and **T** are perpendicular to each other (that is, precisely when $\mathbf{T_2}$ = 0).

7.4   Translation ∗ Glide Reflection

7.4.1 <u>Just an extra translation.</u> This case is so close to the previous one that it hardly deserves its own visual justification. Indeed, let $\mathbf{G} = \mathbf{M*T_0} = \mathbf{T_0*M}$ be the glide reflection, and let **T** be the translation. Then $\mathbf{G*T} = \mathbf{(M*T_0)*T} = \mathbf{M*(T_0*T)}$ and $\mathbf{T*G} = \mathbf{T*(T_0*M)}$ =

($T*T_0$)$*M$. Since $T_0*T = T*T_0$ is again a translation T', we have reduced this section to the previous one; and we may safely say that the composition of a translation and a glide reflection is another glide reflection, with their axes parallel to each other (and **identical** if and only if the translation is **parallel** to the glide reflection).

7.4.2 <u>Could it be a reflection?</u> We have run into compositions of non-parallel translations and glide reflections as far back as 6.2.5 and figure 6.13, while studying two-colored **pg** types: we could even say that the **pg**'s **diagonal** translations are 'responsible' for the perpetual repetition of the **vertical** glide reflection axes! And the interaction between the **pg**'s glide reflection and translation is also reflected in the fact that the only **pg** type ($\mathbf{p_b'1g}$) with both color-reversing and color-preserving glide reflection is the only **pg** type that has color-reversing translation (figures 6.4, 6.9, and 6.11).

But a similar observation is possible about two-colored **cm** types: the two types that have color-preserving reflection and color-reversing glide reflection ($\mathbf{p_c'm}$) or vice versa ($\mathbf{p_c'g}$) are precisely those that do have color-reversing translation (figures 6.25-6.28). Could it be that, the same way the **pg**'s 'diagonal' translation takes us from one 'vertical' glide reflection to another, the **cm**'s 'diagonal' translation takes us from 'vertical' reflection to 'vertical' glide reflection (which is to be expected in view of 7.3.2) **and** from 'vertical' glide reflection to 'vertical' reflection? In broader terms, could the composition of a glide reflection and a translation be **'exactly'** a reflection?

The answer is **"yes"**: a translation and a glide reflection may after all create a reflection! And this may be verified not only in the **cm** examples mentioned above, but also though a visit to our newly painted bathroom wall: for example, the composition $\mathbf{MG_1}*T$ in figure 7.5 is the vertical reflection passing through R_0. How does that happen? A closer look at the interaction between T and the hidden glide reflection $\mathbf{MG_1}$'s gliding vector T_0 is rather revealing:
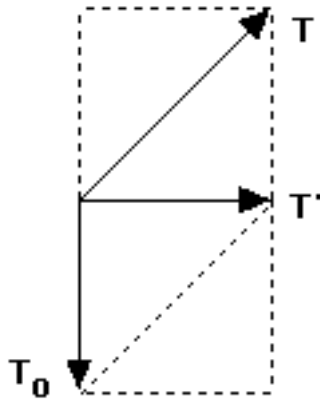
Fig. 7.12

A bit of 'square geometry' in figure 7.12 makes it clear that the composition $\mathbf{T'} = \mathbf{T_0} * \mathbf{T}$ is perpendicular to $\mathbf{T_0}$ (and $\mathbf{MG_1}$ as well). But we have already seen (combining 7.3.2 and 7.4.1) that $\mathbf{G} * \mathbf{T}$ is a reflection if and only if $\mathbf{T'}$ is perpendicular to $\mathbf{G}$: this is certainly the case in figures 7.12 & 7.5 (with $\mathbf{G} = \mathbf{MG_1}$).

In general, what relation between the glide reflection $\mathbf{G}$'s vector $\mathbf{T_0}$ and the translation vector $\mathbf{T}$ is equivalent to $\mathbf{G} * \mathbf{T}$ (and therefore, by 7.3.2, $\mathbf{T} * \mathbf{G}$ as well) being a reflection? A bit of simple trigonometry (figure 7.13) shows that it all has to do with the **lengths** $|\mathbf{T_0}|$ and $|\mathbf{T}|$ of $\mathbf{T_0}$ and $\mathbf{T}$, as well as the **angle** ϕ between $\mathbf{T_0}$ and $\mathbf{T}$. Indeed, all we need is that for the angle $a(\mathbf{T_0}, \mathbf{T'})$ between $\mathbf{T_0}$ and $\mathbf{T'} = \mathbf{T_0} * \mathbf{T}$ to be $\pi/2$ (90^0). But in that case we end up with a **right** triangle of side lengths $|\mathbf{T}|$, $|\mathbf{T_0}|$, and $|\mathbf{T'}|$ and angles $\pi - \phi$ and $\phi - \pi/2$ (figure 7.13); it follows that $|\mathbf{T_0}| = |\mathbf{T}| \times \cos(\pi - \phi) = |\mathbf{T}| \times \sin(\phi - \pi/2)$, so that $|\mathbf{T_0}| = -|\mathbf{T}| \times \cos\phi$ or $|\mathbf{T}| = -|\mathbf{T_0}|/\cos\phi$, where, **inevitably**, $\pi/2 < \phi \leq \pi$.
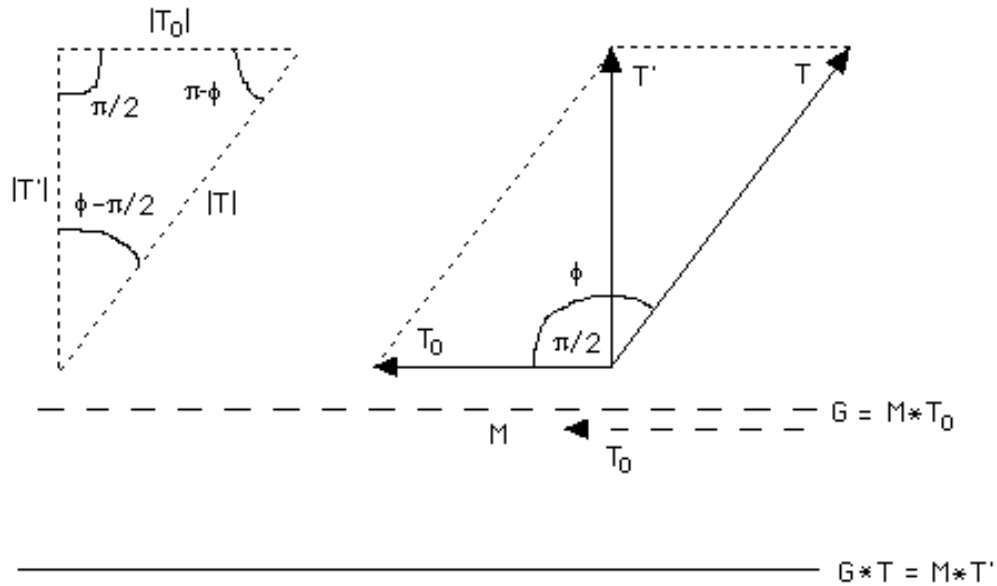
Fig. 7.13

So, to 'annul' the vector T_0 of a glide reflection $G = M*T_0$, all we need is to 'multiply' G by a translation T of length $|T|$ that makes an angle ϕ with T_0 such that $|T_0| = -|T|\cos\phi$. Observe that $\cos\phi < 0$, hence ϕ has to be an obtuse angle (forcing T to go 'somewhat opposite' of T_0); also, in view of $|T| = -|T_0|/\cos\phi$, the closer ϕ is to $\pi/2$ the longer T is: $\pi/2 < \phi \leq \pi$ yields $|T_0| \leq |T| < \infty$, with $|T| = |T_0|$ corresponding to $\phi = \pi$ ($T = T_0^{-1}$ and $G*T = T*G = M$ -- the rather obvious 'parallel case').

In figures 7.12 & 7.5, $\phi = 135^0$ and $|T| = -|T_0|/\cos(135^0) = |T_0|\sqrt{2}$.

7.5   Rotation $*$ Rotation

7.5.1 <u>Just like two reflections?</u> Counterintuitive as it might seem as first, it turns out that determining the composition of two rotations is about as easy as determining the composition of two reflections. And you will be even more surprised to see that the key to the puzzle lies inside figure 7.10 (that does not seem to have anything to do with rotations)! On the other hand, a figure that is

certainly related to rotations is 7.9: we demonstrated there how the composition of two intersecting reflections is a rotation; in this section we will play the game backwards, **breaking** rotations into two intersecting reflections.

So, let's first consider two clockwise rotations $R_A = (A, \phi_1)$ and $R_B = (B, \phi_2)$. To compute R_B*R_A we set $R_A = M*L$ and $R_B = N*M$, where **L**, **M** are reflection lines intersecting each other at A at an angle $\phi_1/2$ and **M**, **N** are reflection lines intersecting each other at B at an angle $\phi_2/2$; in particular, **M** is the line defined by A and B (figure 7.14), the **common reflection** destined to play the same **'vanishing'** role as in 7.3.1 (and figure 7.10). It is easy now to determine $R_B*R_A = (N*M)*(M*L) = N*L$ as a **rotation** centered at C (composition of two reflections intersecting each other at C).
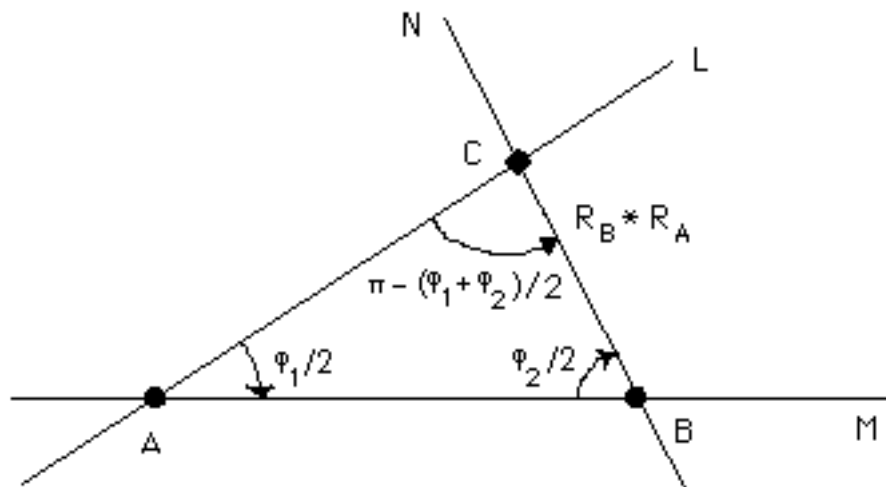
Fig. 7.14

So, it was quite easy to determine R_B*R_A's center, and there is nothing 'special' about it. But there is another potential surprise when it comes to R_B*R_A's angle: although both R_A and R_B are taken clockwise, $R_B*R_A = N*L$ ends up being counterclockwise (going from **L** toward **N**)! How about R_A*R_B then, with each of R_A and R_B taken counterclockwise this time? Or R_B*R_A with one rotation taken clockwise and the other counterclockwise, and so on? Taking **both** order and orientation into account, there exist eight possible cases

(all based on **M**'s 'elimination'), shown in figure 7.15 (arguably the most important one in the entire chapter or even book):
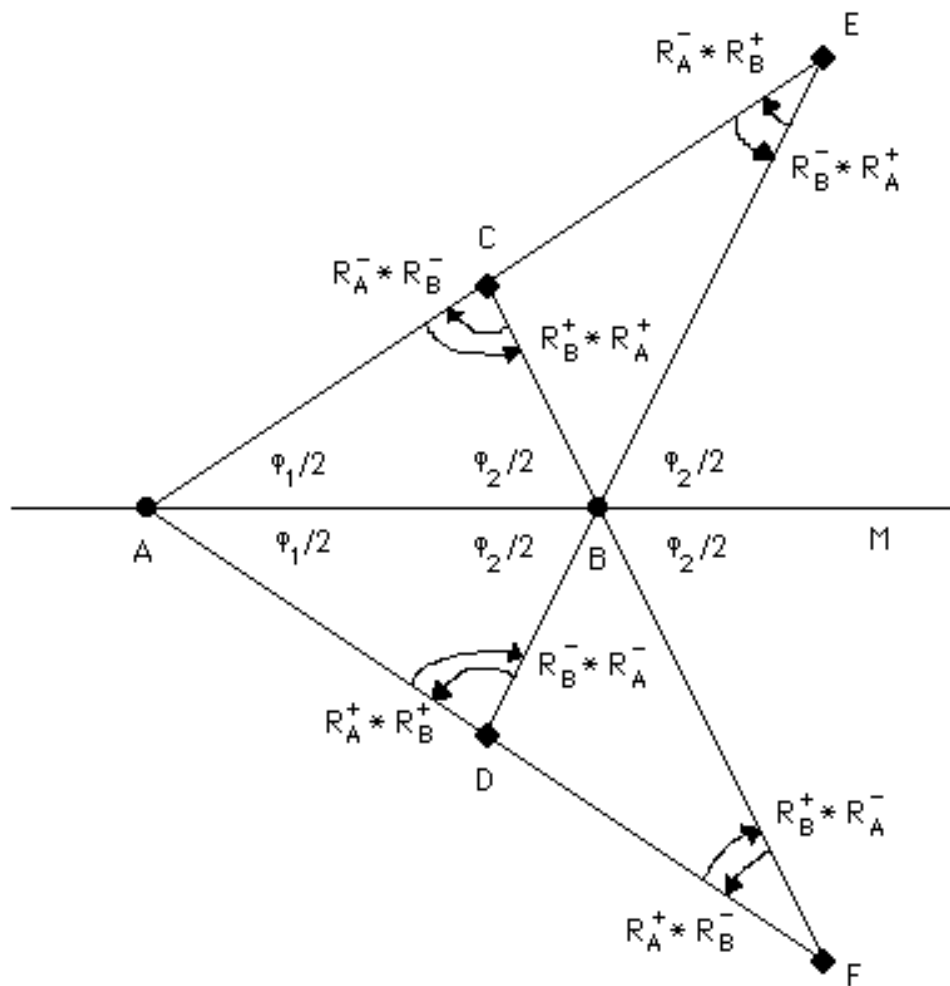

Fig. 7.15

As in 7.0.4, clockwise rotations are marked by a **+** superscript and counterclockwise rotations are marked by a **-** superscript, while the **arrows** pointing to each composition angle indicate its orientation. The example shown in figure 7.14 is therefore $R_B^+ * R_A^+$; notice how each of the four centers C, D, E, F is **shared** by two compositions. Notice that the four rotations centered at C and D have angles equal to $2 \times \angle ACB = 2 \times (180^0 - (\phi_1 + \phi_2)/2) = 360^0 - \phi_1 - \phi_2$, which is **equivalent** to $\phi_1 + \phi_2$ (with **reversed** orientation, via $\phi_1 < 180^0$ and $\phi_2 < 180^0$); and the four compositions centered at E and F have angles equal to $2 \times \angle CFA = 2 \times (180^0 - \angle CAF - \angle ACF) = 2 \times (180^0 - \angle CAD - \angle ACB) =$

$2\times(180^0-\phi_1-(180^0-(\phi_1+\phi_2)/2)) = 2\times(-(\phi_1/2)+(\phi_2/2)) = \boldsymbol{\phi_2-\phi_1}$ (which would have been $\boldsymbol{\phi_1-\phi_2}$ in case ϕ_1 was bigger than ϕ_2).

7.5.2 <u>When the angles are equal.</u> When $\boldsymbol{\phi_1 = \phi_2}$, our preceding analysis suggests that the angle between AE and BE (or AF and BF) in figure 7.15 is zero; but AE and BE are certainly **distinct**, passing through two distinct points A and B: indeed the two lines, making equal angles with **M**, should be **parallel** to each other, with E and F 'pushed' all the way to **infinity**! In simpler terms, when two rotations $\boldsymbol{R_A}$, $\boldsymbol{R_B}$ have **equal** angles of **opposite** orientation (one clockwise, one counterclockwise) their composition is a **translation** (composition of parallel reflections, see 7.2.1). [Notice (figure 7.15) that E and F act as centers precisely for those product rotations where one factor is counterclockwise and the other one is clockwise.]

Of course we do not need something as complicated and thorough as figure 7.15 to conclude that the composition of two rotations of equal, opposite angles is a translation: a simple modification of figure 7.14 suffices!
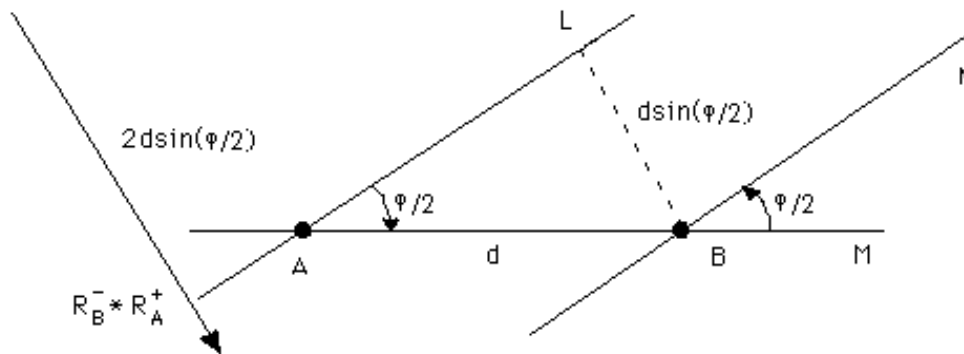
Fig. 7.16

With $\boldsymbol{R_A^+} = (A, \phi) = \boldsymbol{M*L}$ and $\boldsymbol{R_B^-} = (B, \phi) = \boldsymbol{N*M}$, **L** and **N** become parallel to each other (figure 7.16), therefore $\boldsymbol{R_B^-*R_A^+} = \boldsymbol{N*L}$ is a translation perpendicular to them (7.2.1). And since the distance between **L** and **N** is $|AB|\sin(\phi/2) = d\sin(\phi/2)$ (figure 7.16), the length of the translation vector is $2d\sin(\phi/2)$.

Once again, viewing a translation as a rotation the center of which is that mysterious 'point at infinity' (3.2.5) turns out to make a lot of sense!

7.5.3 <u>The case of half turn.</u> There is another way of destroying the **quadrangle** of figure 7.15: reduce it to a **triangle** by forcing the lines DE and CF to be one and the same, which would happen if and only if they are both perpendicular to **M** at B, that is if and only if $\phi_2 = \mathbf{180^0}$. Other than reducing the number of product rotations from eight to four, and the number of intersection points (rotation centers) from four to two, making one of the two rotations a half turn would not have any other consequences. But if **both** rotations are 180^0 then there are **no intersections** at all, and the number of compositions is further reduced from four to two: with angle orientation no longer an issue, both $\mathbf{R_A * R_B}$ and $\mathbf{R_B * R_A}$ are now **translations** of vector length 2d (figure 7.16 with $\phi = 180^0$).

7.5.4 <u>An important example.</u> How about the 'surviving' rotations of figure 7.15 when $\phi_1 = \phi_2$? Let's look at the case $\phi_1 = \phi_2 = \mathbf{60^0}$, where two sixfold centers at A and B generate counterclockwise and clockwise rotations of $\phi_1 + \phi_2 = \mathbf{120^0}$ at C and D (figure 7.17), as well as four translations that we will not be concerned with. With **M**, **N**, and **L** as in figure 7.14, and **N′**, **L′** being the mirror images of **N**, **L** about **M**, the four 120^0 rotations may be written as **N∗L**, **L′∗N′** (clockwise) and **L∗N**, **N′∗L′** (counterclockwise). Everything is shown in figure 7.17, and it is clear that the four centers A, B (60^0) and C, D (120^0) form a **rhombus**.
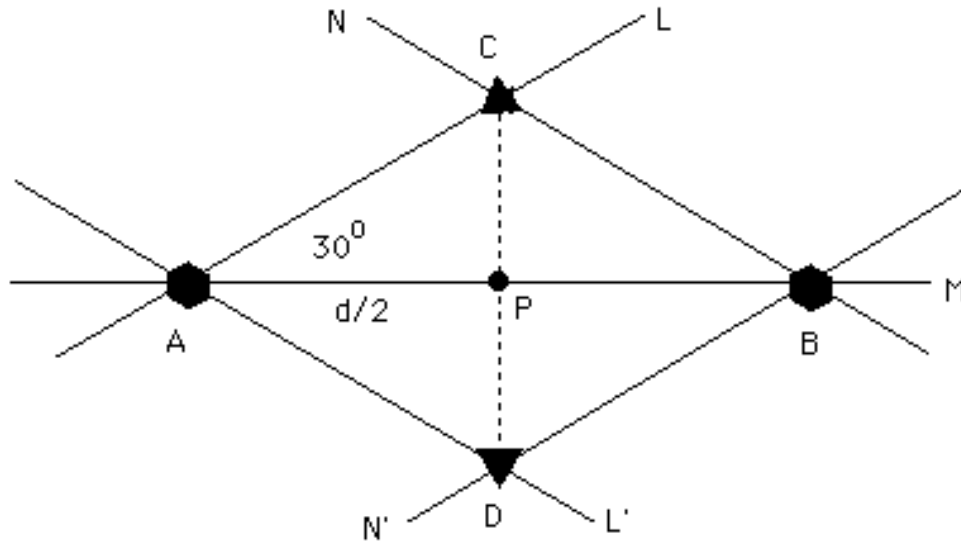
Fig. 7.17

So, any two sixfold centers A, B are bound to create two threefold centers C, D -- **but not vice versa**! What is the location of C (or D) with respect to A and B? With $|AB| = d$ and P the midpoint of AB, simple trigonometry in PAC establishes $|PC| = |AP|\tan 30^0 = d/(2\sqrt{3})$. It follows that $|CD| = d/\sqrt{3}$ and $|AD| = |AC| = \sqrt{|PA|^2 + |PC|^2} = \sqrt{d^2/4 + d^2/12} = d/\sqrt{3}$: the triangle ACD is **equilateral**! (Notice that ACBD will be a rhombus whenever $\phi_1 = \phi_2$, but ACD (and BCD) will be equilateral **if and only if** $\phi_1 = \phi_2 = 60^0$.)

All this begins to look rather familiar: didn't we talk about that rhombus of sixfold centers when we classified two-colored **p6m** types (6.17.3 & 6.17.4, figures 6.134-6.138)? The two rhombuses are **similar**, except that the one in 6.17.3 consists of **four** sixfold centers, while the one we just produced involves **two** sixfold and **two** threefold centers: where does the 6.17.3 rhombus come from? To answer this question, we simply adapt the quadrangle of figure 7.15 with $\phi_1 = 60^0$ and $\phi_2 = 120^0$; that is, we determine the 'total combined effect' of a sixfold center (A) and a threefold center (B), shown (figure 7.18) in the context of the **beehive**:
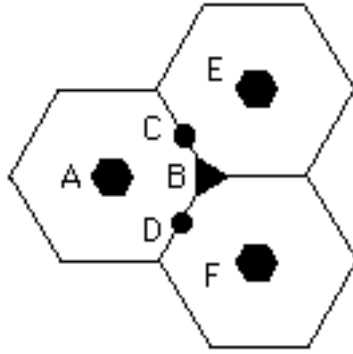
Fig. 7.18

Starting with centers A and B as above we produced two **180⁰** ($\phi_1+\phi_2$) centers (C and D) and two **60⁰** ($\phi_2-\phi_1$) centers (E and F). So, now we have three sixfold centers: where is the **fourth** one? Well, the answer lies in a combination of figures 7.17 and 7.18: sixfold centers E and F are bound (figure 7.17) to produce another threefold center B′, mirror image of B about EF; and then E (or F) and B′ will have to create the 'missing' sixfold center A′, A's mirror image about EF -- in the same way A and B produce E (and F) in figure 7.18!

Let's summarize the situation a bit: we may 'start' with two sixfold centers that create two threefold centers (figure 7.17), hence two additional sixfold centers (figure 7.18 plus discussion); or 'start' with one sixfold center and one threefold center that create two additional sixfold centers (figure 7.18), hence another threefold center (figure 7.17), and then a fourth sixfold center (figure 7.18 again). It seems rather clear that the first approach, summarized in figure 7.19 below, makes more sense:

Fig. 7.19

Notice that we have removed not only the labels of the various centers, but the beehive as well: indeed, since we have created its

lattice using **only** sixfold rotations, the lattice created in figure 7.19 is **also** the rotation center lattice of a **p6**; after all, the **p6** and the **p6m** are no different when it comes to their lattices of rotation centers (6.16.1).

The process of figure 7.19 can go on to create the full lattice shown in figure 4.5 (right); the next step involves compositions of **'peripheral'** sixfold and twofold centers, generating new threefold centers. The only question that remains is: could we have 'started' with **only one** sixfold center instead of two? The answer is "yes", provided that we seek some help from **translation**: as figure 7.18 shows, F is E's image under the pattern's **minimal** vertical translation (**T**); and, following 4.0.4 (Conjugacy Principle), **T**(E) = F **has** to be a sixfold center! [Attention: as in 4.0.4 again, **T**(E) is not the same as **T**∗**E** or **E**∗**T**, where **E** stands for the sixfold rotation(s) centered at E; we do **not** need **compositions** of translation and rotation (studied in the next section) to 'create' the beehive's lattice -- but we **do** need them to 'create' the bathroom wall's lattice (7.6.3)!]

7.6   Translation ∗ Rotation

7.6.1 <u>A trip to infinity.</u> What happens as A moves further and further westward in figure 7.14? Clearly **L** becomes 'nearly parallel' to **M** and the rotation angle ϕ_1 approaches zero; 'at the limit', when A has 'reached infinity', **L** and **M** are **parallel** to each other and the clockwise rotation R_A = **M**∗**L** becomes a **translation T** = **M**∗**L**:
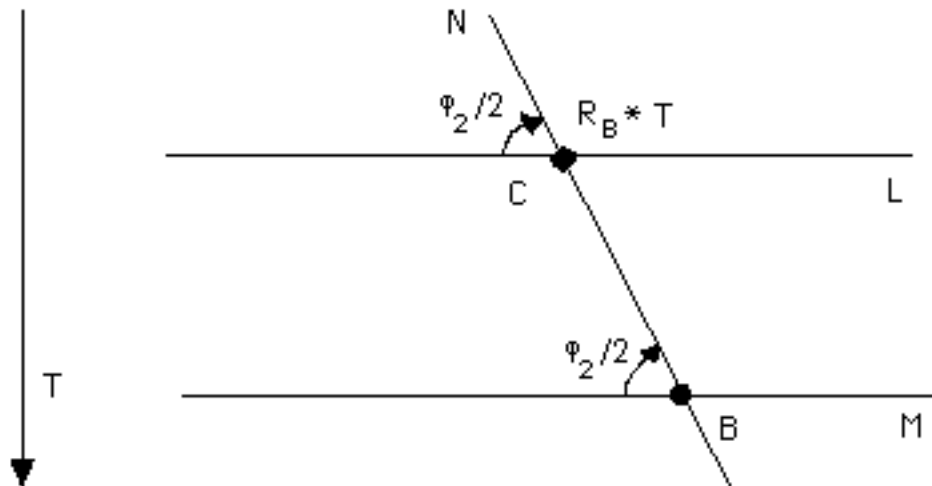
Fig. 7.20

Just as in figure 7.14, and with $R_B = N*M$ still a clockwise ϕ_2 rotation, the composition $R_B*T = N*L$ is now a **clockwise** rotation, centered at C, the point of intersection of **N** and **L**. Since **L** and **M** are parallel to each other, the angle between **L** and **N** is still $\phi_2/2$, therefore R_B*T's angle remains equal to ϕ_2. As for the location of R_B*T's center, that is fully determined via $|BC| = |T|/(2\sin(\phi_2/2))$, a relation that has in essence been derived in figure 7.16.

7.6.2 <u>Our old example.</u> How does 7.6.1 apply to the composition $T*R_0$ of 7.0.3? We demonstrate this below, in the context of figure 7.1, blending into it figure 7.20:
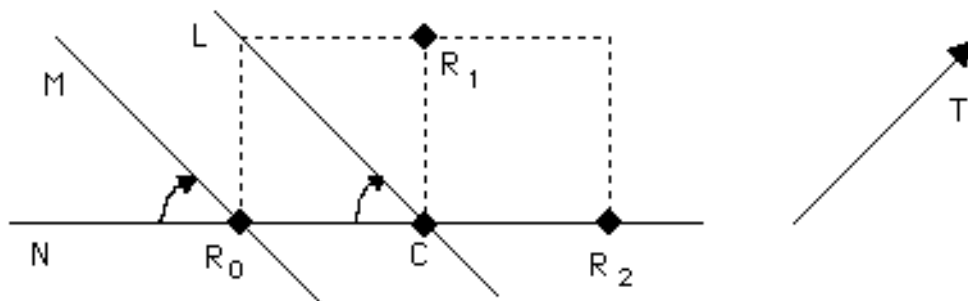
Fig. 7.21

With clockwise $R_0 = M*N$ and $T = L*M$, $T*R_0$ is equal to $L*N$, a

clockwise 90^0 rotation centered at C, intersection point of **L** and **N**.

7.6.3 <u>An important pentagon.</u> So, we have established that the composition of a translation **T** and a rotation **R** = (K, φ) is again a rotation by φ about another center. But, just as we did in 7.5.1, we observe here that the final outcome of the composition depends on the order in the operation (**R∗T** versus **T∗R**), the rotation's orientation (**R** clockwise versus **R** counterclockwise), and the translation's sense (**T** versus **T⁻¹**). Again, there exist **eight** possible combinations sharing **four** rotation centers (C, D, E, F), all featured in figure 7.22 (that parallels figure 7.15, with **R**$_A$ replaced by **T**):
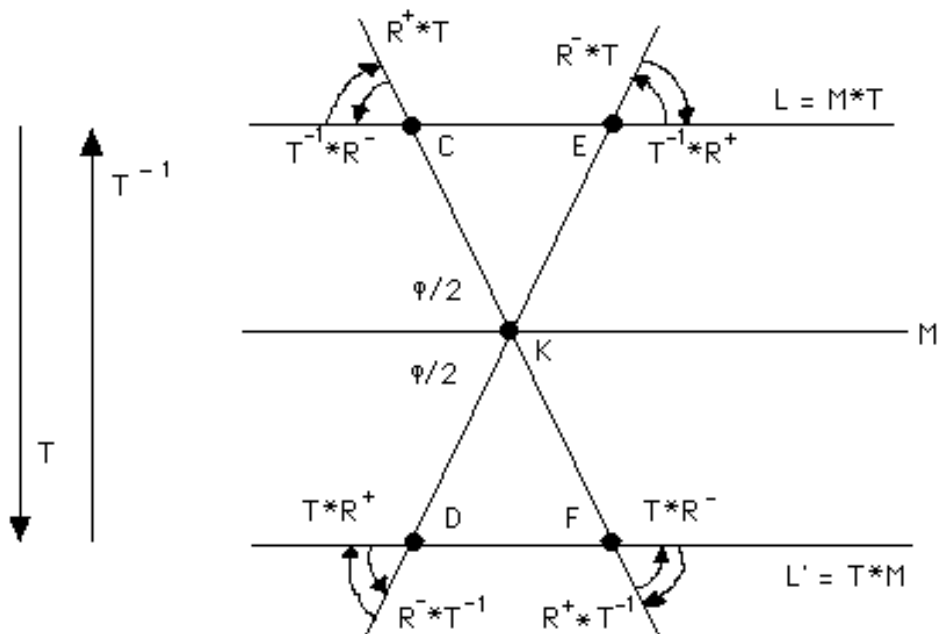
Fig. 7.22

As in figure 7.15, each angle's orientation is indicated by arrows pointing to it; all rotation angles are equal to φ, a fact that may be derived from our findings in 7.5.1 (with ϕ_1 = 0 and ϕ_2 = φ), of course.

The five rotation centers (K, C, D, E, F) in figure 7.22 form a very symmetrical, non-convex **'pentagon'** -- a more 'scientific' term is *quincunx* -- that may remind you of the number **5**'s standard representation on **dice**! We have already seen it, certainly without noticing, in figure 7.19 (right): over there it stands for a 'formation' of twofold centers in a **p6** lattice, all of them obtained as

compositions of 'higher' rotations. Should that lattice have been allowed to grow further, we would have certainly seen similar pentagons formed by sixfold centers, as well as rectangles formed by threefold centers; see also figure 4.2, and figure 7.25 further below. All those **p6** centers had been obtained by way of composition of **rotations**, starting from two sixfold centers -- or, if you prefer, **one** sixfold center and an image of it under translation. Now we derive the **p4** and the **p3** lattices of rotation centers **starting** from a 'pentagon': that is, we start with **one** fourfold or threefold rotation and **compose** it with the pattern's **minimal 'vertical'** translation, in the spirit of figure 7.22.

First, the **p4** lattice, shown initially in its '**Big Bang**' (pentagonal) stage, then with some twofold centers created by the fourfold centers, and, finally, with additional fourfold centers created by one fourfold and one twofold center:
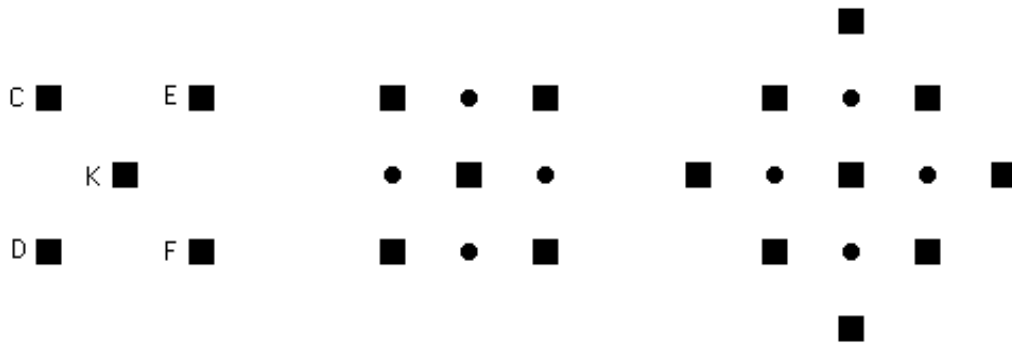
Fig. 7.23

Next comes the **p3** lattice, where threefold centers keep creating nothing but threefold centers:
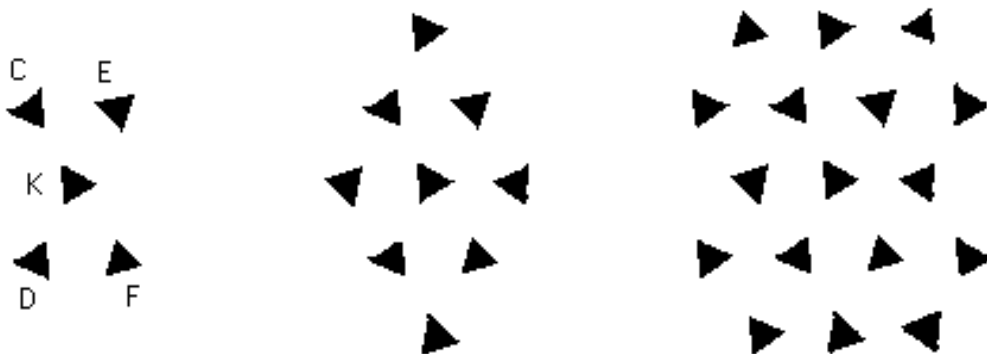
Fig. 7.24

How do these lattices relate to the ones shown in figures 4.59 (**p4**) and 4.68 (**p3**)? Looking at their 'fundamental pentagon' KCDEF (figure 7.22) in the context of those figures, as well as figures 7.23 & 7.24, we observe the following: the **p4** pattern has no translation taking K to any of the other four vertices, but it certainly has translations interchanging any two vertices among C, D, E, F (**'two kinds'** of fourfold centers, as indicated in figure 4.59); and the **p3** pattern has no translation interchanging any vertices from the 'first column' (C, D) with any vertices from either the 'third column' (E, F) or K (**'three kinds'** of threefold centers, as indicated in figure 4.68). Notice that these observations are fully justified by the pentagon's very 'creation': vector CD is by definition the pattern's **minimal** translation, and this rules out vector KF (but certainly **not** vector CF) in the case of **p4** (figure 7.23, left); CD's minimality also rules out vector CE (**hence** vector CF as well, for CE = CF−CD) in the case of **p3** (figure 7.24, left)!

Let's now look at the **p6**'s 'first three stages of creation', composing the 'first' rotation with a translation (as in the cases of **p4** and **p3**, figures 7.23 and 7.24, respectively) rather than another rotation (as in figure 7.19):
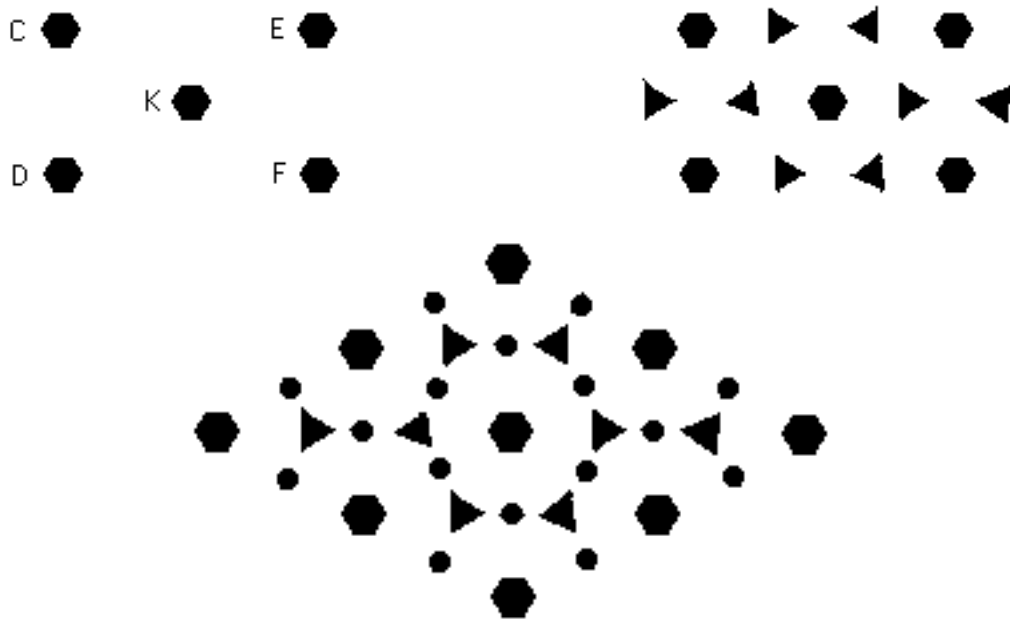
Fig. 7.25

This is of course an **alternative** way of looking at **p6**'s lattice: you can't miss the **four** copies of the rhombus in figure 7.19 packed inside the big rhombus of figure 7.25! But more illuminating is figure 7.25's pentagon, showing that there exists only **'one kind'** of sixfold centers: observe how any two of its vertices (labeled as in figure 7.22 always) are interchangeable via one of the **p6**'s translations -- indeed all edges but CE (and DF) are **'equivalent'** to either CD or 2×CD, while the above noticed CE = CF−CD allows CE (and DF) as well.

7.6.4 <u>When the pentagon collapses.</u> Exactly as in 7.5.3 and figure 7.15, a 180^0 rotation would make lines DE and CF one and the same in figure 7.22, allowing for only **one** intersection (and half turn center) with each of **L** and **L′**. So, $\phi = 180^0$ makes a trio of **collinear** points (C $\equiv$ E, K, D $\equiv$ F, with |KC| = |KD| = |**T**|/2) out of the pentagon of figure 7.22. And yet there exists a 'starting pentagon' in every **p2** pattern, created by **one** half turn **R** and **two** non-parallel translations T_1, T_2:
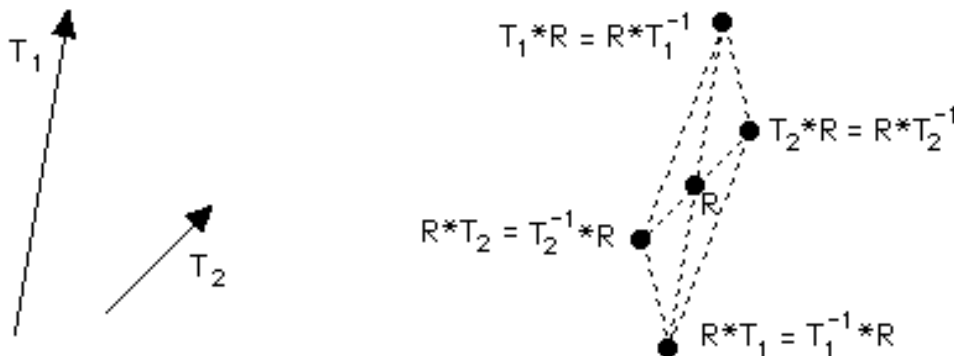
Fig. 7.26

We leave it to you to check the details in figure 7.26 and extend its **'oblique'** pentagon into the full **p2** lattice of half turn centers; keep in mind that many **new** half turn centers may **only** be created with the help of **translations**: after all the composition of any two half turns is a translation, not a half turn (7.5.3)!

Notice the importance of having two non-parallel, **'minimal'** translations available in the case of the **p2** pattern: assuming existence of translation in **one** direction only, plus 180^0 rotation, we are only guaranteed a **p112** (border) pattern -- half turn centers

endlessly multiplied by the translation along a single line! On the other hand, the pentagon of rotation centers created by one threefold (**p3**) or fourfold (**p4**) or sixfold (**p6**) rotation and one minimal translation is bound (7.5.2) to produce translations in **three** (and eventually infinitely many) additional directions.

7.7   Rotation ∗ Reflection

7.7.1 <u>When the center lies on the mirror.</u> A comparison between the previous two sections shows that rotation and translation are of rather similar mathematical behavior. This is of course due to the fact that each of them is the composition of two reflections, a fact that also lies behind the proximity of this section and section 7.3; in particular, figure 7.27 below may be seen as a **'copy'** of figure 7.10:
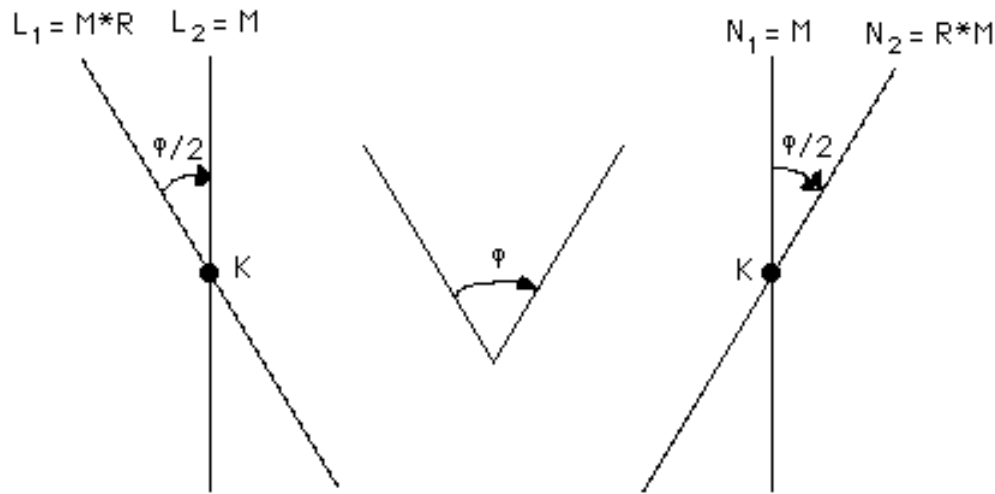
Fig. 7.27

On the left is the composition **M∗R** of a **clockwise** rotation **R** = (K, φ) followed by a reflection **M**, while on the right is **R∗M**; as figure 7.27 makes it clear, **R**'s center K lies on **M**. As in section 7.3 and figure 7.10, we analysed **R** as $L_2 * L_1$ with L_2 = **M** in the first case, and as $N_2 * N_1$ with N_1 = **M** in the second case; in both cases **M** cancels out, exactly as in figure 7.10.

Adopting (as in previous sections) the notations R^+ and R^- for **R**

taken clockwise and counterclockwise, respectively, we observe (in the context of figure 7.27 always) that $M*R^+ = R^-*M = L_1$ and $M*R^- = R^+*M = N_2$. So, the composition of a rotation and a reflection passing through the rotation center is always another reflection **'tilted'** by half the rotation angle, and still passing through the rotation center.

7.7.2 <u>The general case.</u> What happens when the rotation center does not lie on the reflection axis? This one looks a bit complicated! Perhaps some initial experimentation, in the context of a four-colored beehive this time, might help:
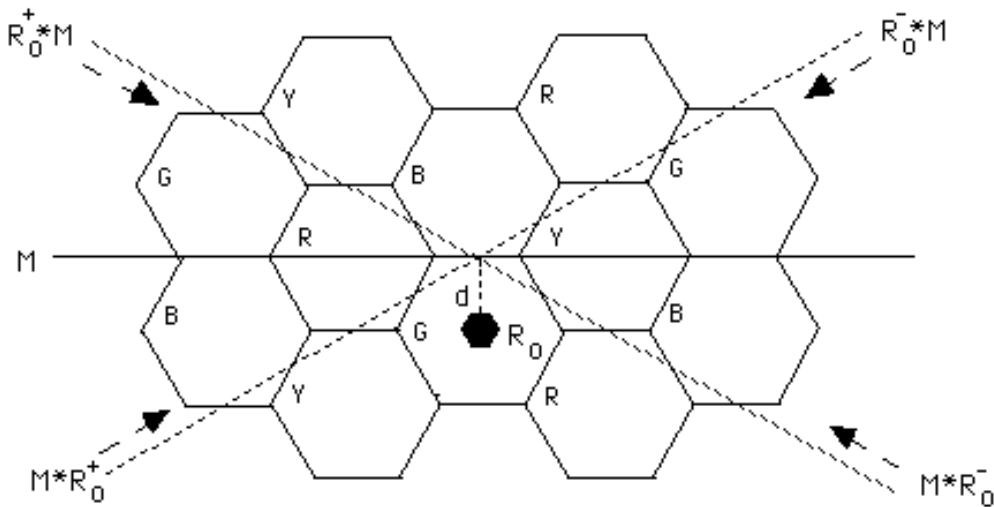
Fig. 7.28

Employing the methods of 7.0.3-7.0.4 if necessary, you may derive all **four** possible combinations between the reflection **M** and the sixfold rotation R_0 in figure 7.28: they are **glide reflections** of gliding vectors of equal length, their **two** axes being mirror images of each other about **M**; at a more subtle level, observe how, in all four cases, the vector's **sense** is such that the glide reflection and the rotation **'turn the same way'**.

Let's now **justify** the outcome of the compositions in figure 7.28 through a specific example of the type R^+*M, where $R^+ = (K, \phi^+)$ and K **not** on **M** (figure 7.29). We write $R^+ = L_2*L_1$, where L_1 is now

parallel to **M**, so that $R^+*M = (L_2*L_1)*M = L_2*(L_1*M) = L_2*T$, where **T** is a translation **perpendicular** to **M**, going from **M** toward L_1 and of length **twice** the distance d between K and **M** (7.2.1).
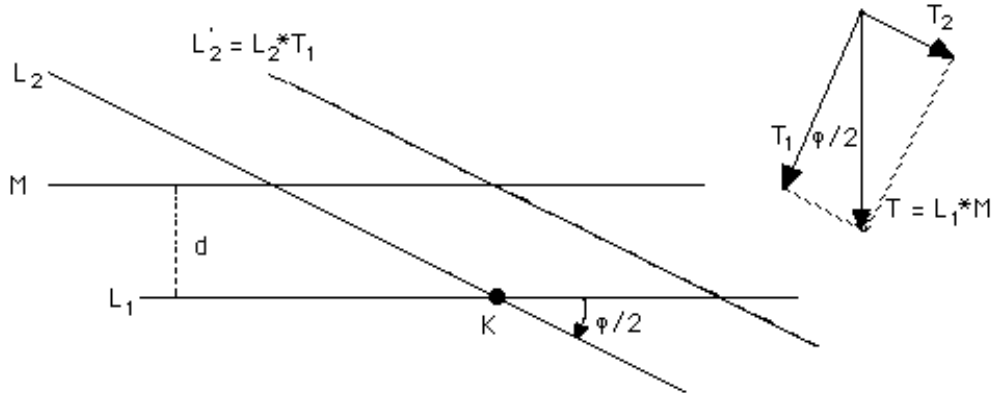
Fig. 7.29

From here on, we appeal to section 7.3: we write $T = T_1*T_2$ with T_1 **perpendicular** to L_2 and T_2 **parallel** to L_2 (7.3.2), so that L_2*T_1 is a reflection L_2' parallel to L_2 and at a distance $|T_1|/2$ from it and 'backward' with respect to T_1 (7.3.1); it follows at long last that $R^+*M = L_2*T = L_2'*T_2$ is indeed a glide reflection (of axis L_2' and vector T_2). Since $a(T, T_1) = a(L_1, L_2) = \phi/2$ (because **T**, T_1 are perpendicular to L_1, L_2, respectively), T_2's length is $|T| \times \sin(\phi/2) = 2d \times \sin(\phi/2)$: you may verify this in the case of figure 7.28, with $\phi = 60^0$ and $|T_2| = d = r\sqrt{3}/2$, where r is the regular hexagon's side length.

7.7.3 <u>A sticking intersection point.</u> Figure 7.29 makes it visually clear that the intersection point of **M** and L_2' is K's projection on **M**. And figure 7.28 provides further evidence: the two glide reflection axes' **common** point is none other than R_0's projection on **M**! But how do we **prove** this fact? The proof is a bit **indirect**: starting from the four lines of figure 7.29, we let B be the point where the **perpendicular** to **M** at A (**intersection point** of **M** and L_2') intersects L_2 (figure 7.30); and then we prove that B **has** to be the **same** as K (intersection point of L_1 and L_2) by showing |AB| to
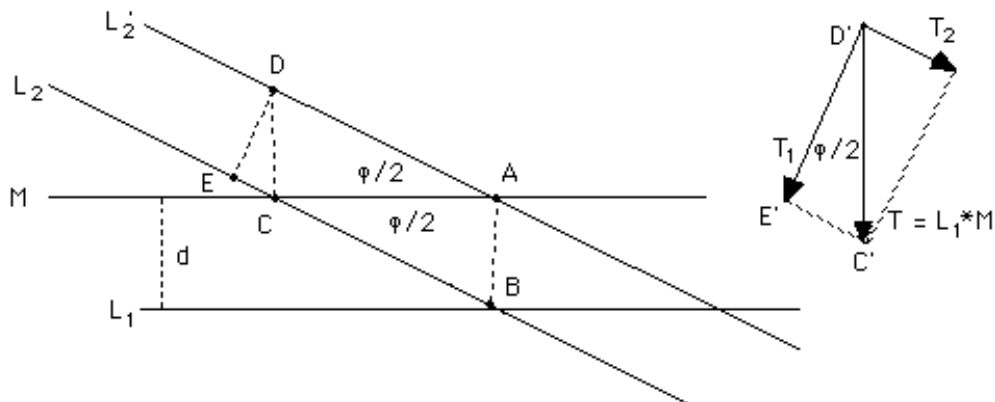
be equal to d (and **implying** that B lies on **L₁**, too)!

Fig. 7.30

To do this, we need two more lines: a line **perpendicular** to **M** at C (**M**'s intersection point with **L₂**), intersecting **L′₂** at D; and a line **perpendicular** to **L′₂** at D that intersects **L₂** at E. Perpendicularities show then the angle CDE to be equal to $\angle$CAD = ϕ/2 and the two right triangles EDC and E′D′C′ to be **similar** (figure 7.30). It follows that $\dfrac{|DE|}{|DC|} = \dfrac{|D'E'|}{|D'C'|}$, so that $|DC| = \dfrac{|DE| \times |D'C'|}{|D'E'|} = \dfrac{(|T_1|/2) \times (2d)}{|T_1|} = d$. Now ABCD is by **assumption** (**L′₂** is parallel to **L₂**, hence AD is parallel to BC) and **construction** (both AB and CD are perpendicular to **M**, hence parallel to each other) a **parallelogram**, therefore |AB| = |CD| = d.

We can finally state that the composition of a rotation **R** = (K, ϕ) and a reflection **M** at a distance d from K is a glide reflection **G** of axis passing through K's projection on **M** and gliding vector of length $2d \times \sin(\phi/2)$, intersecting **M** at an angle $\phi/2$.

7.7.4 <u>Could it pass through the center?</u> Figures 7.28 & 7.29 may for a moment give you the impression that the glide reflections produced by the combination of a rotation and a reflection cannot possibly pass through the rotation center: once again the case of **half turn** comes as a surprise! Not as a complete surprise though, as this situation (where the two glide reflection axes of figure 7.28 become one and the same) is characteristic of the **pma2** and **pmg**

patterns, where 'vertical' reflections 'multiplied' by half turns produce 'horizontal' glide reflection(s) passing through their centers: at long last, our **'two as good as three'** observations in 2.6.3 begin to make full sense!

Notice, along these lines, that the relations **M∗R = G** and **R∗M = G^{-1}**, where **R** is a **half turn**, yield (by way of 'multiplication' of each side by **R** and **M**, respectively, and **R^2 = M^2 = I**) the relations **G∗R = M = R∗G^{-1}** and **M∗G = R = G^{-1}∗M**: these represent special cases of the next two sections and also illuminate further, if not completely, the structure of the **pma2** and **pmg** patterns!

7.8   Rotation ∗ Glide Reflection

7.8.1 <u>Just a bit of extra gliding.</u> First a rather familiar example:
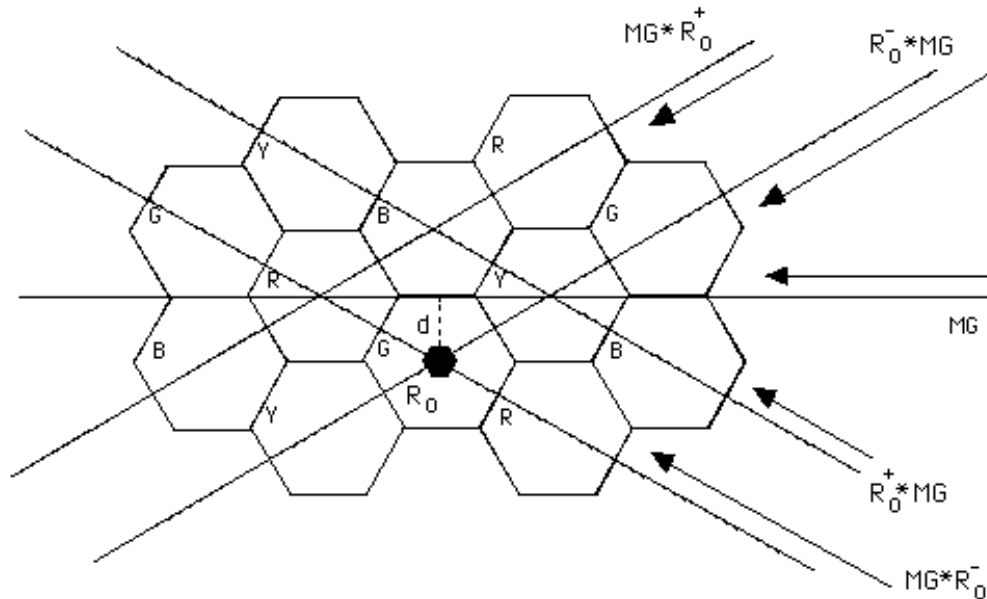
Fig. 7.31

What went on? There has been some slight **'disturbance'** of figure 7.28, hasn't it? All we did was to replace the reflection **M** by the hidden glide reflection **MG**, and then ... the glide reflection axes got scattered away from the safety of **R$_0$**'s projection onto **M** ... into the four points of the horizon -- in fact two of them ended up

passing through R_0 itself, despite the rotation being 60^0 rather than 180^0 (7.7.4)!

To get a better understanding of the situation, it would be helpful to see what happens when **MG** is replaced by its inverse:
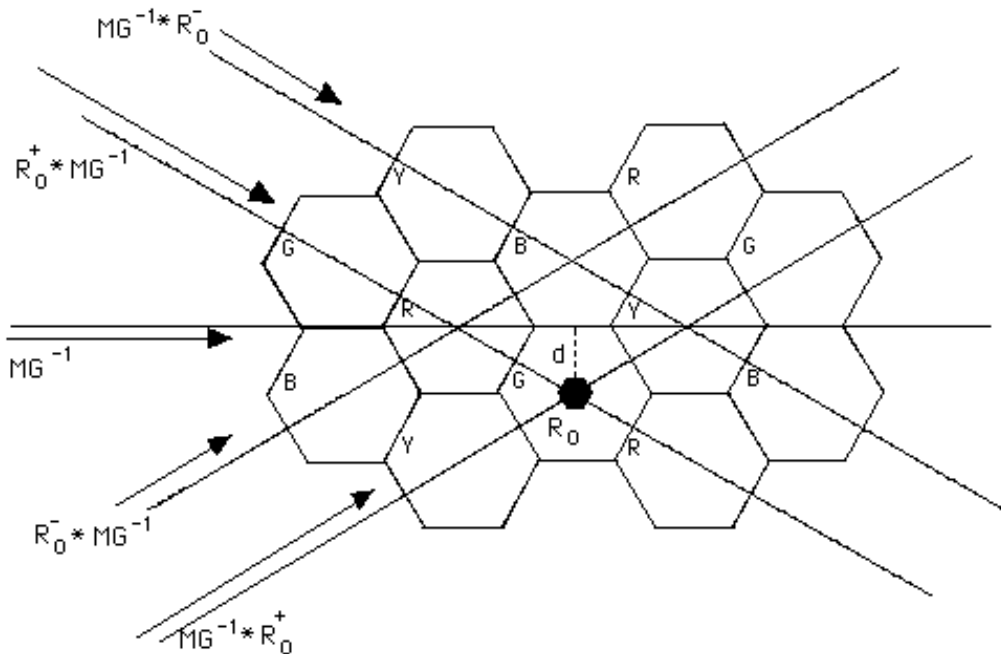

Fig. 7.32

In case that was not already clear through the comparison of figures 7.28 and 7.31, figure 7.32 certainly proves that the glide reflection vector has **'the last word'**: that should be intuitively obvious, and we go on to articulate it right below.

Let **R** be the rotation, and **G** = **M∗T** = **T∗M** the glide reflection. Then **R∗G** = (**R∗M**)**∗T** and **G∗R** = **T∗**(**M∗R**), where **R∗M** and **M∗R** are glide reflections: this section is just a blending of sections 7.4 and 7.7!

As an example, let us illustrate how we went from the **M∗R$_0^+$** of figure 7.28 (section 7.7) to the **MG∗R$_0^+$** = **T∗**(**M∗R$_0^+$**) of figure 7.31:
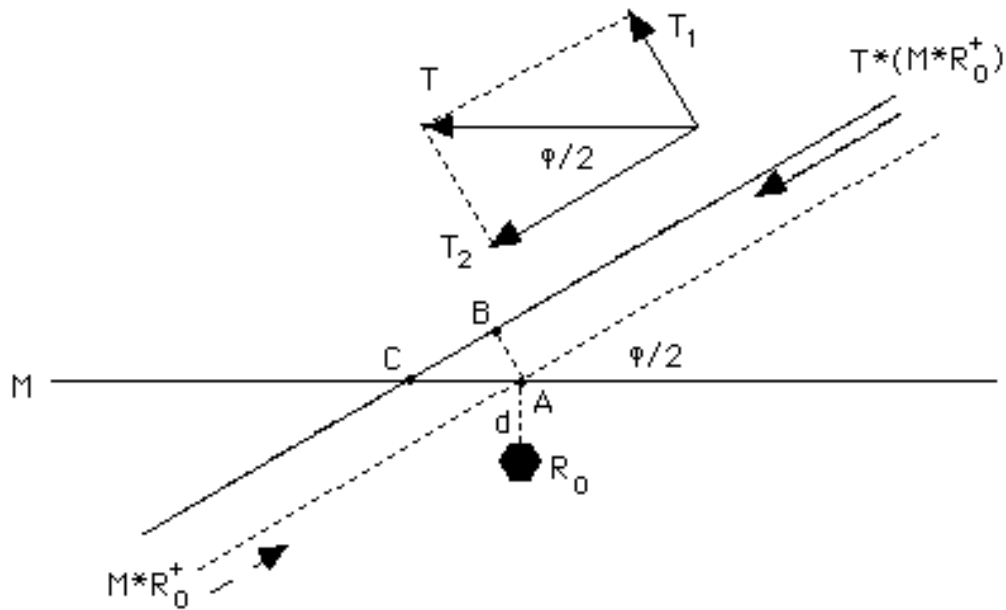
Fig. 7.33

All we had to do was to apply the idea of figure 7.11 and analyse **MG**'s gliding vector **T** into two vectors: one perpendicular to $M*R_0^+$ (T_1) that pulls $M*R_0^+$'s axis **'forward'** by $|T_1|/2$ (7.3.1), and one parallel to $M*R_0^+$ (T_2) that is easily **added** to $M*R_0^+$'s vector (of **opposite** to T_2's sense in this case); the outcome is the glide reflection of figure 7.33, which is no other than figure 7.31's $MG*R_0^+$, of course.

Figure 7.33 illustrates clearly why the glide reflection axes of figures 7.31 & 7.32 are still **parallel** to the glide reflection axes of figure 7.28, still making angles of 30^0 with **M**. Moreover, figure 7.33 determines exactly **where** they cross **M**: $|AC| = |AB|/(\sin(\phi/2)) = (|T_1|/2)/(\sin(\phi/2)) = ((|T|\sin(\phi/2))/2)/(\sin(\phi/2)) = |T|/2$. (That's why the distance between the two **'crossing points'** in figures 7.31 & 7.32 is **equal** to $|T|$ and, may we add, **independent of** ϕ!) Finally, figure 7.33 explains why there are vectors of two **distinct** lengths, $|T| \times \cos(\phi/2) + 2d \times \sin(\phi/2)$ and $||T| \times \cos(\phi/2) - 2d \times \sin(\phi/2)|$, in figures 7.31 & 7.32: $M*R_0^+$ and $M*R_0^-$ have gliding vectors of **equal length** $2d \times \sin(\phi/2)$ (7.7.2) but **distinct direction**, and the latter forces distinct lengths for the gliding vectors of $T*(M*R_0^+)$ and $T*(M*R_0^-)$; to recall our 'cryptic' expression from 7.7.2 (as well as

7.0.4), the longer vector is produced when the glide reflection and the rotation **'turn the same way'**.

7.8.2 <u>Could it be a reflection?</u> In the important special case where the glide reflection axis passes through the rotation center, $d = 0$ implies gliding vectors of length $|T| \times \cos(\phi/2)$ for **all four** resulting glide reflections; their intersecting axes will still form a **rhombus** (as in figures 7.31 & 7.32), but the rotation center (R_0) will now be in the **middle** of that rhombus (like fourfold center **D** combined with glide reflection G_4 in figure 6.106 (**p4g**), for example). But the rhombus disappears when $\phi = 180^0$! In partial 'compensation', $|T| \times \cos(180^0/2) = 0$ turns the glide reflections into **two** reflections crossing the original glide reflection at a distance of $|T|/2$ from the half turn center: in case you didn't realize, that's the **pmg**'s story!

In general, when does a rotation turn a glide reflection into a reflection? Recall that we asked a similar question in 7.4.2: the answer remains the same here, and so does the way to get it. Indeed, with $R*G = (R*(M*T_1))*T_2$ and $G*R = T_2*((T_1*M)*R)$, all we need is for T_2 to be of **sense opposite** of $R*(M*T_1)$'s (or $(T_1*M)*R$'s) gliding vector (which is **bound** to happen for either **G** or G^{-1}) **and** of **equal length** to it. Focusing on the latter condition, and referring to figure 7.33 and 7.7.2, we see that all we need is the equality $|T| \times \cos(\phi/2) = 2d \times \sin(\phi/2)$ -- trivially valid in the case of **pmg** (with $d = 0$ and $\phi = 180^0$) and equivalent to $|T| = 2d \times \tan(\phi/2)$ when $\phi \neq 180^0$.

Of course we have already seen an example of $R*G = M$ in 7.0.4 and figure 7.5, where $R_3^-*G_1 = M_1$: assuming that each tile has side length 1, $|T| = 2d \times \tan(\phi/2)$ holds with $|T| = \sqrt{2}/2$, $d = \sqrt{2}/4$ and $\tan(\phi/2) = \tan 45^0 = 1$. So, it is possible for the composition of a 90^0 rotation and a **'diagonal'** glide reflection to produce a reflection in the case of a **p4m** pattern; this also happens in the **p4g** pattern, as you should be able to verify (in figure 4.55 for example).

7.9 Reflection * Glide Reflection

7.9.1 <u>Only two centers.</u> In the **pmg** pattern, the combination of a reflection **M** and a glide reflection **G** perpendicular to each other produces **two** half turns the centers of which lie on **G**'s axis and are **mirror images** of each other about **M**: this may either be checked directly (and by appeal to the discussions in 7.7.4 and 7.8.2 if necessary) or be derived as a special case of figure 6.6.2 (by making **one** of the glide reflection vectors zero). Could this be due to the **right angle**'s 'special privileges'? After all, there exist **four** possibilities altogether (**M*G**, **G*M**, **M*G^{-1}**, **G^{-1}*M**) that could create four distinct centers. Well, a look at 7.0.4 and figure 7.6 is not that promising for center diversity: over there we established $M_1*G_1 = R_4^-$ and indicated that $G_1*M_1 = R_5^+$, with M_1 a 'horizontal' reflection and G_1 a 'diagonal' glide reflection in a **p4m** pattern (bathroom wall); and a bit more work would show that $M_1*G_1^{-1} = R_5^-$ and $G_1^{-1}*M_1 = R_4^+$ -- only **two** centers altogether!

Evidence for two rather than four centers is strengthened by a more 'exotic' (**p31m**) example:
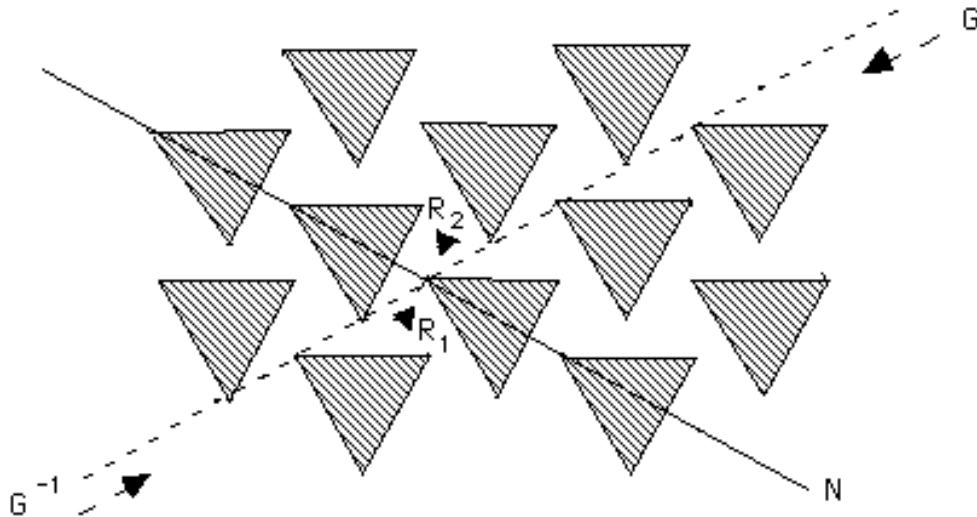
Fig. 7.34

You should be able to verify $N*G = R_2^+$, $G*N = R_1^-$, $N*G^{-1} = R_1^+$, and

$G^{-1}*N = R_2^-$: again, **four** compositions sharing **two** centers. (Notice here that R_1 and R_2 are among the **p31m**'s '**off-axis**' 120^0 centers (4.16.1), derived through the compositions above rather than as obvious compositions of intersecting reflections.)

7.9.2 <u>The way to the two centers.</u> Having 'only' two centers would make sense not only in view of the examples presented, but also in view of what we saw in 7.7.2: the combination of a reflection and a rotation produced two, not four, glide reflection axes. Moreover, having two rather than four centers will make perfect sense after the '**whole story**' is revealed in section 7.10!

So, having resigned to living with just two centers, how do we find them? How would we justify figure 7.34? Using M_1 instead of N and setting $G = M_2*T = T*M_2$, $G^{-1} = M_2*T^{-1} = T^{-1}*M_2$, we notice that the four compositions of figure 7.34 may be written as $(M_1*M_2)*T$, $T*(M_2*M_1)$, $(M_1*M_2)*T^{-1}$, and $T^{-1}*(M_2*M_1)$; now M_1*M_2 and M_2*M_1 are rotations R^+, R^- of same center K and angle ϕ (120^0 in this case) but opposite orientation, so we may '**blend**' figures 7.34 and 7.22:
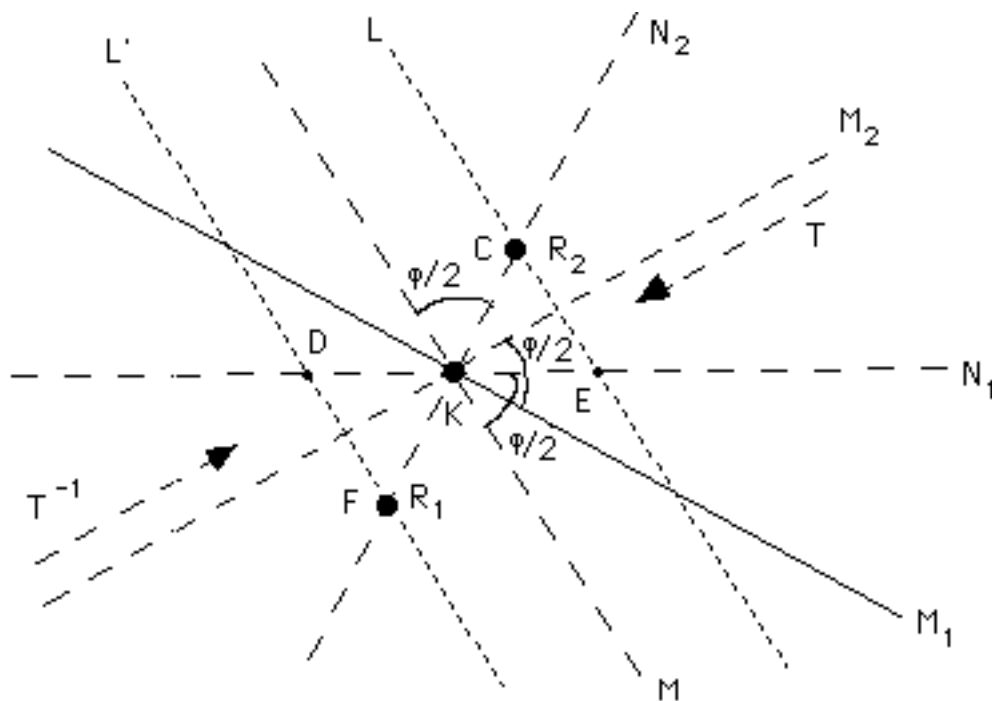
Fig. 7.35

So, with N_1 = DE, N_2 = CF, M perpendicular to T (therefore M_2 as well), L and L' parallel to M with d(M, L) = d(M, L') = $|T|/2$, and a(M, N_1) = a(M, N_2) = a(M_1, M_2) = 60^0 ($\phi/2$), the 'blending' of figures 7.22 and 7.34 is complete: center R_1 (figure 7.34) corresponds to F (figure 7.22) and the rotations $R^+*T^{-1} = (M_1*M_2)*T^{-1} = N*G^{-1}$ and $T*R^- = T*(M_2*M_1) = G*N$; and center R_2 (figure 7.34) corresponds to C (figure 7.22) and the rotations $R^+*T = (M_1*M_2)*T = N*G$ and $T^{-1}*R^- = T^{-1}*(M_2*M_1) = G^{-1}*N$. And there is a **bonus** as well: observe, focusing on **acute** angles always, that a(M_1, N_2) = a(M_1, M_2) + a(M_2, N_2) = a(M, N_2) + a(M_2, N_2) = a(M, M_2) = 90^0! In other words, M_1 and N_2 are **perpendicular** to each other: this is going to be important both in 7.9.3 below and in section 7.10.

Our analysis above has certainly explained how the composition centers are born, but there is one more question to answer: what do **'unused centers'** D (intersection of L' and N_1) and E (intersection of L and N_1) of figure 7.35 stand for? The answer is: they represent rotations **unrelated** to the given pair of reflection and glide reflection (and **not** 'belonging' to the **p31m** pattern of figure 7.34)! For example, one of the two rotations based on E is $R^-*T = (M_2*M_1)*T = M_2*(M_1*T)$, which is the composition of **another pair** of reflection (M_2) and, by 7.3.2, glide reflection (M_1*T); it is of course crucial that we cannot replace M_2*M_1 by M_1*M_2 (7.2.3).

7.9.3 <u>A 'practical guide'.</u> The detailed discussion in 7.9.2 is certainly enlightening, but how would you describe to someone not terribly interested in mathematical rigor the **general** procedure for determining the composition of a reflection and a glide reflection? To be more precise, how would you lead that person to the center of the resulting rotation? That's really the only crucial question: for it is clear from the preceding discussion that the rotation angle is **twice** the **intersection angle** of the reflection and the glide reflection; and, once the center is known, the angle's orientation is easy to determine (by checking what happens at the **intersection point** of the reflection and the glide reflection, for example).

Removing all 'redundant information' from figure 7.35, we arrive at an easy answer to our question. Indeed, since N_2 is perpendicular to M_1 (7.9.2) and L, L' are perpendicular to M_2 with the intersection point K half way from L to L' (figure 7.35), the procedure for determining the rotation centers R_1, R_2 for the four possible compositions of 7.9.1 is simple: pick points K_1, K_2 on M_2 so that $|KK_1|$ = $|KK_2|$ = $|T|/2$, and then draw lines L', L perpendicular to M_2 at K_1, K_2 respectively, and line N_2 perpendicular to M_1 at K; R_1 and R_2 are now determined as the intersections of N_2 by L and L' (figure 7.36).
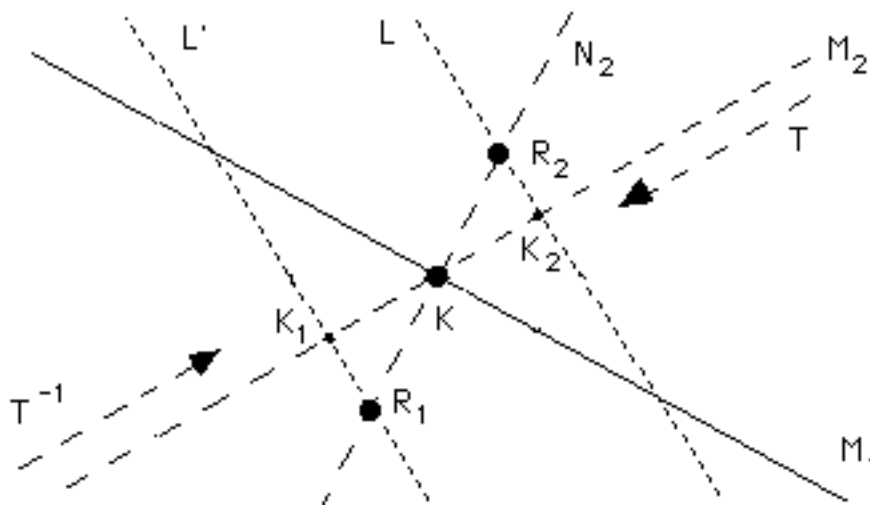
Fig. 7.36

Of course figure 7.36 **alone** does not tell us which center (between R_1, R_2) to use for any given combination of reflection and glide reflection. Some rules can be derived by referring to the discussion following figure 7.35, or perhaps by looking at figure 7.40 in section 7.10. But it is probably easier to follow the tip given above and determine the right center and angle orientation simply by checking where the intersection of the two axes is mapped. We illustrate all this in figure 7.37 below, where we verify the identities $M_1 * G_1 = R_4^-$ and $G_1 * M_1 = R_5^+$ of figure 7.6 (bathroom wall), which is reproduced in part, explicitly demonstrating the determination of centers R_4 and R_5: looking at the pair K, $M_1 * G_1(K)$, it becomes clear that the only rotation among R_4^+, R_4^-, R_5^+, R_5^- that

could map K to $M_1*G_1(K)$ is R_4^-, therefore $M_1*G_1 = R_4^-$; likewise, looking at the pair K, $G_1*M_1(K)$, we conclude that $G_1*M_1 = R_5^+$.
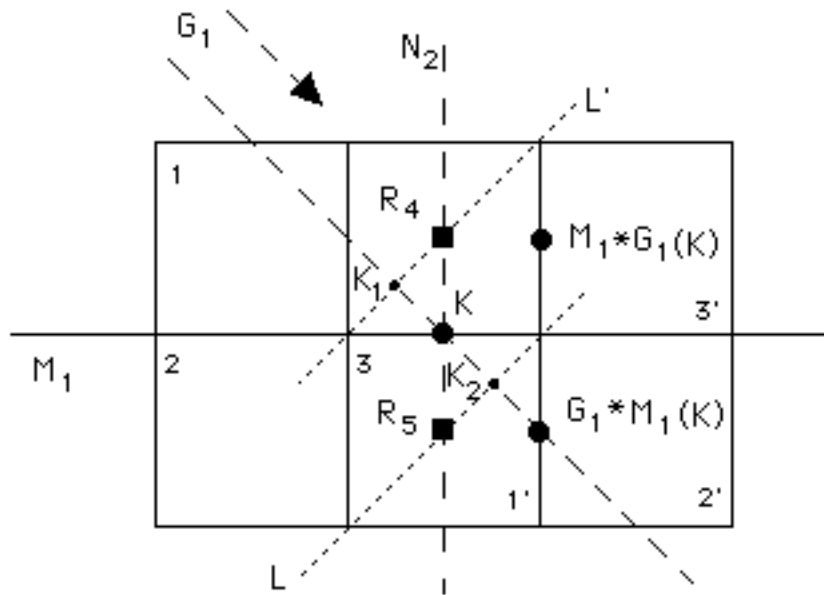

Fig. 7.37

7.9.4 <u>When the axes are parallel.</u> Everything we discussed so far in this section collapses in case M_1 and M_2, that is N and G are parallel to each other. Luckily, the compositions $N*G = (M_1*M_2)*T$ and $G*N = T*(M_2*M_1)$ are much easier to determine in this case; we derive these **translations** below, leaving $N*G^{-1}$ and $G^{-1}*N$ to you:
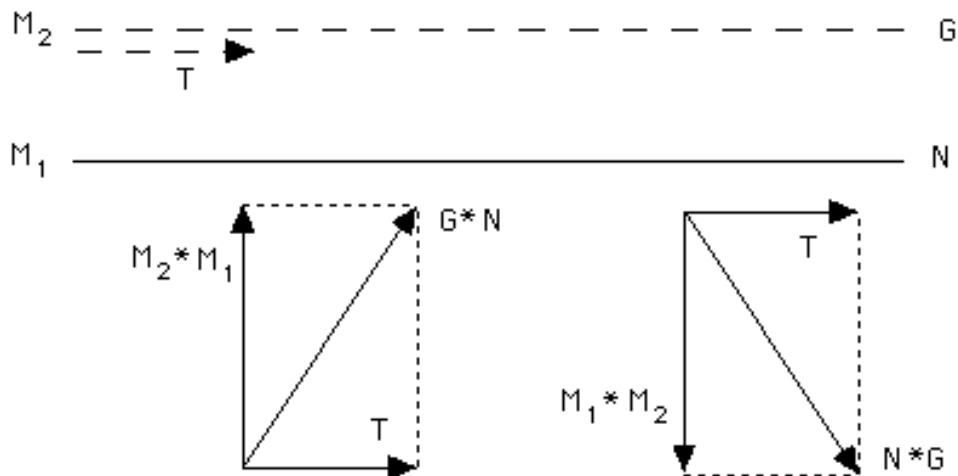

Fig. 7.38

Of course all this is strongly reminiscent of sections 7.3 and 7.4; and such compositions are prominent in **cm** (and **pm**) patterns, as well as all patterns containing them: **more** on this in chapter 8!

7.10   Glide reflection $*$ Glide Reflection

7.10.1 <u>Parallel axes.</u> This '**pg**' case is similar to the '**cm**' case of 7.9.4. Indeed $G_1*G_2 = T_1*(M_1*M_2)*T_2 = (T_1*T_2)*(M_1*M_2)$ and $G_2*G_1 = T_2*(M_2*M_1)*T_1 = (T_2*T_1)*(M_2*M_1)$ are '**diagonal**' translations:
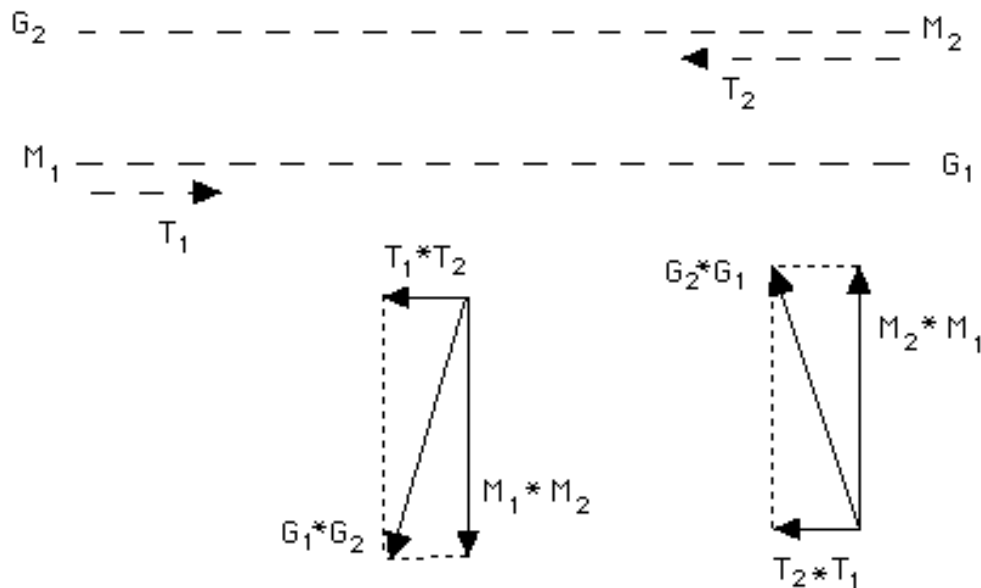
Fig. 7.39

Notice that the special case $T_1 = -T_2$ (with $T_1*T_2 = I$) has been employed in 6.3.2 (figure 6.21) in our investigation of two-colored **pm** patterns.

7.10.2 <u>A good guess indeed!</u> We now come to the much more involved case where G_1 and G_2 intersect each other at a point K. Luckily, most of the work has **already** been done in section 7.9!

Indeed, had you been asked to determine G_1*G_2 (etc) yourself, you would probably look at figure 7.36 and think like this: "were M_1 a glide reflection $G_1 = M_1*T_1$ instead of a mere reflection, I would have treated it exactly as $G_2 = M_2*T_2$; that is, I would draw lines N, N' perpendicular to M_2 and at a distance of $|T_2|/2$ to the left and right of K, and then I would look for the rotation center(s) at their intersection(s) with L' and L"; and surely you would already know that the composition is a **rotation** by an angle **twice** the intersection angle of G_1 and G_2! And you would be right on the mark:
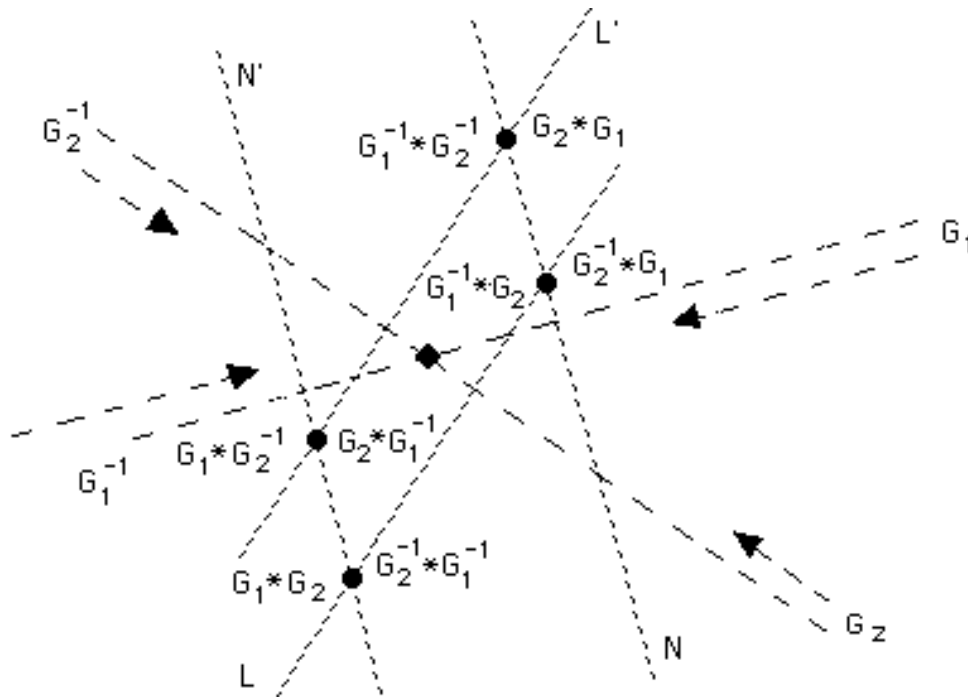

Fig. 7.40

Figure 7.40 offers an **exhaustive** overview of the situation, covering all **eight** possible combinations and **four** rotation centers: it is possible to develop rules about **'what goes where'**, but it is probably **smarter** to do what we suggested in 7.9.3 (and figure 7.37) when it comes to determining rotation centers and angle orientation!

In simple terms, draw two perpendiculars at each of the two axes and at distances equal to half the length of the respective gliding vector on each side of their intersection point, then look for the four intersections of the resulting two pairs of parallel lines

(figure 7.40): observe that this **generalizes** figure 6.54, where the two axes are **perpendicular** to each other!

7.10.3 Where do they come from? Notice how we have **upgraded** from the two possible centers of figure 7.36 to the four possible centers of figure 7.40: this is hardly surprising if you notice that we did get an extra translation here (as the reflection turned into glide reflection) and if you recall how the addition of a translation increased the number of glide reflection axes from two (figure 7.28, **R∗M**) to four (figures 7.31 & 7.32, **R∗G**).

In 7.8.1, and figure 7.33 in particular, we explained how the additional translation leads to the two extra axes (when the reflection (figure 7.28) combined with the rotation is **upgraded** to glide reflection (figures 7.31 & 7.32)). We do something similar in figure 7.41 below, showing how **each** of the two rotation centers (R_1, R_2) generates **two** new rotation centers (R_4, R_5 and R_3, R_6, respectively), the **same way** K generated R_1 and R_2 in figure 7.36:
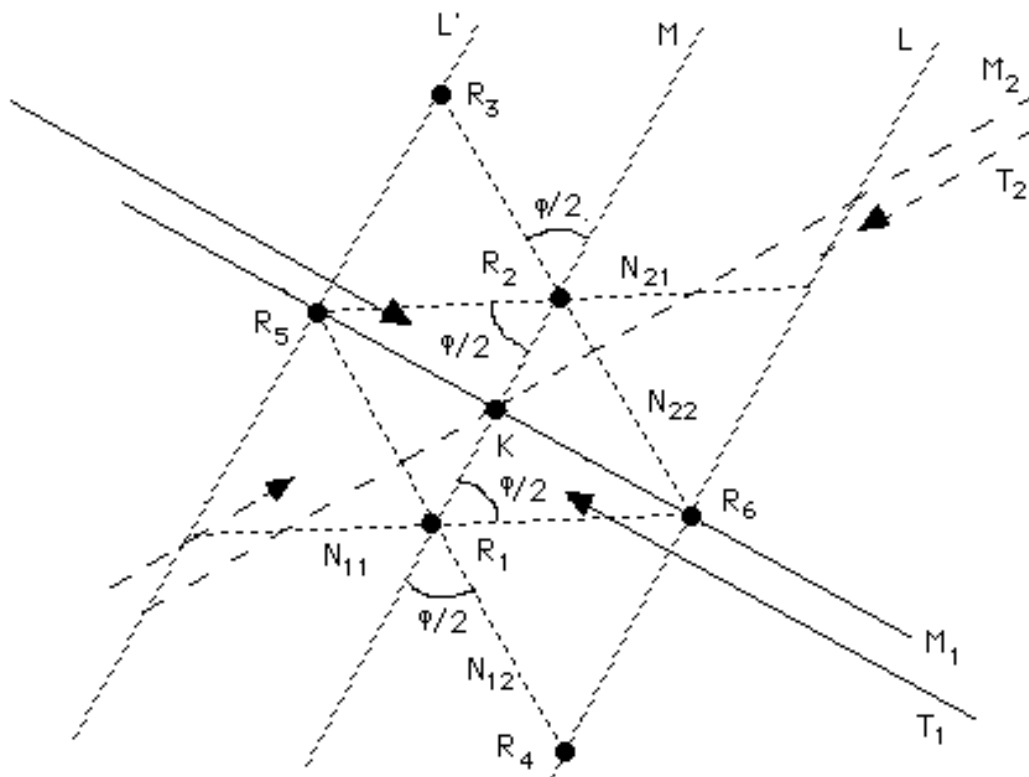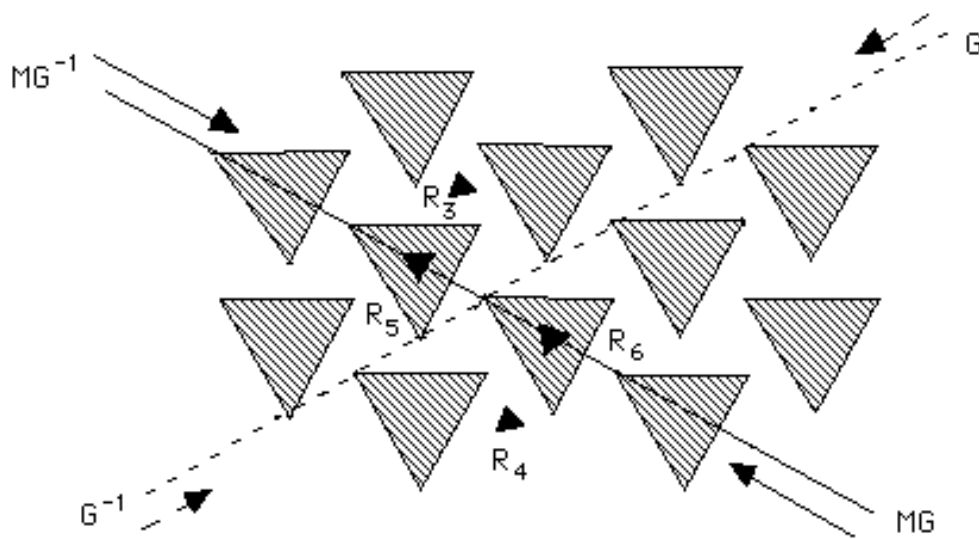

Fig. 7.41

Basically, all we had to do was to combine each of **R$_1$** and **R$_2$** with the **'added'** translation **T$_1$**, exactly as in figures 7.22 **and** 7.35; and, for the same reason that line **N$_1$** was **'useless'** in figure 7.35, lines **N$_{11}$** and **N$_{21}$** play no role in figure 7.41: our rotation centers are created by the intersections of lines **N$_{12}$** and **N$_{22}$** with **L** and **L′**. (Notice however that **R$_5$ also** lies on **N$_{21}$**, while **R$_6$ also** lies on **N$_{11}$**: this is part of a **'coincidence'** discussed right below.)

Are you ready for a little **surprise**, at long last? Figure 7.41 is in fact an **'abstract detail'** of a **familiar** piece, namely figure 7.34! Indeed **M$_2$∗T$_2$** is figure 7.34's glide reflection **G**, while **M$_1$∗T$_1$** is figure 7.34's reflection **N** upgraded to a hidden glide reflection **MG**; everything is fully revealed in figure 7.42:

$$MG*G = R_3^+, \; G*MG = R_4^-, \; MG*G^{-1} = R_5^+, \; G^{-1}*MG = R_6^-,$$
$$G^{-1}*MG^{-1} = R_3^-, \; MG^{-1}*G^{-1} = R_4^+, \; G*MG^{-1} = R_5^-, \; MG^{-1}*G = R_6^+$$

Fig. 7.42

So, the 'coincidence' mentioned above reflects on the fact that **R$_5$** and **R$_6$** are **'on-axis'** 120^0 centers in figure 7.34's **p31m** pattern: figure 7.42 indicates that those centers are generated whenever two **'somewhat opposite'** glide reflections are combined; but it is

more crucial to find out **'why'** those centers fall on the axes, and we do that next as a byproduct of a broader investigation.

7.10.4* Some coordinates, at long last! Our goal here is to determine the **location** of the four rotation centers (A, B, C, D) corresponding to 'all possible combinations' of the two given glide reflections **G₁, G₂ analytically** -- that is, using **cartesian coordinates** (for the first time since chapter 1)! To do that, we **'rotate'** figure 7.40 so that **G₁** is now our **x-axis** ($y = 0$), while **G₂** is a line of unspecified **slope m** ($y = mx$), and the intersection point of **G₁, G₂** is the **origin** (0, 0); we also set $|T_1| = 2d_1$ and $|T_2| = 2d_2$, so that the perpendiculars to **G₁**, **N** and **N′**, are now represented by the equations $x = d_1$ and $x = -d_1$, respectively (figure 7.43).
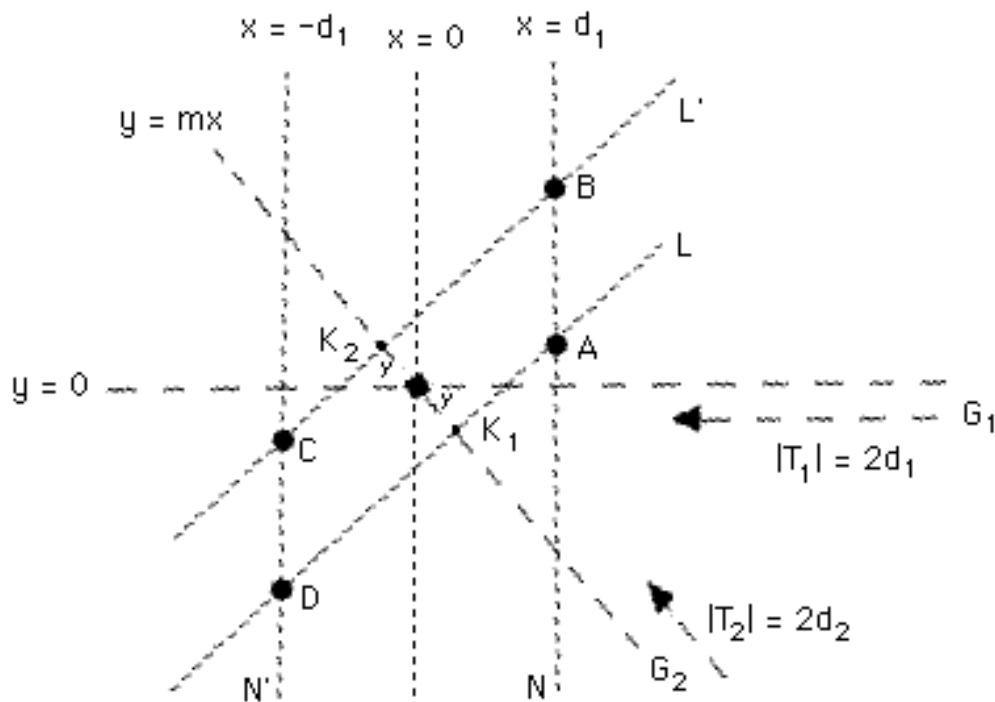

Fig. 7.43

The critical step is to determine the equations of the lines **L** and **L′**: being perpendicular to $y = mx$ and **symmetric** of each other about (0, 0), they may be written as $y = (-1/m)x - k$ and $y = (-1/m)x + k$, respectively; k is a real number that we need to determine, and we

do so by first determining the coordinates of K_1 and K_2, the intersection points of **G_2** with **L** and **L'**, respectively (figure 7.43).

Solving the systems **y = mx = (−1/m)x + k** and **y = mx = (−1/m)x − k**, we obtain $K_1 = (\dfrac{-km}{m^2+1}, \dfrac{-km^2}{m^2+1})$ and $K_2 = (\dfrac{km}{m^2+1}, \dfrac{km^2}{m^2+1})$. We know that $|K_1K_2| = 2d_2$, so the **distance formula** leads to

$$\sqrt{(\dfrac{-km}{m^2+1} - \dfrac{km}{m^2+1})^2 + (\dfrac{-km^2}{m^2+1} - \dfrac{km^2}{m^2+1})^2} = 2d_2,$$ which is equivalent to

$$\dfrac{4k^2m^2}{(m^2+1)^2} + \dfrac{4k^2m^4}{(m^2+1)^2} = 4d_2^2, \quad \dfrac{k^2m^2}{m^2+1} = d_2^2 \text{ and, finally, } \mathbf{k = \pm\dfrac{d_2}{m}\sqrt{m^2+1}}.$$

Knowing now the equations of **L** $(y = (-1/m)x - (d_2/m)\sqrt{m^2+1})$ and **L'** $(y = (-1/m)x + (d_2/m)\sqrt{m^2+1})$, it is **trivial** to determine the coordinates of their intersections with **N** $(x = d_1)$ and **N'** $(x = -d_1)$:

$$\mathbf{A = (d_1, \dfrac{-d_1-d_2\sqrt{m^2+1}}{m}), \quad B = (d_1, \dfrac{-d_1+d_2\sqrt{m^2+1}}{m}),}$$

$$\mathbf{C = (-d_1, \dfrac{d_1+d_2\sqrt{m^2+1}}{m}), \quad D = (-d_1, \dfrac{d_1-d_2\sqrt{m^2+1}}{m}).}$$

Now we can finally answer the question: when does the center of a rotation that is the composition of two glide reflections lie on one of the glide reflection axes? Working in the context of figure 7.43, always, we notice that there exist **two** distinct possibilities: two centers lying on **G_1** (if and only if their y-coordinate is 0), and two centers lying on **G_2** (if and only if their coordinates x and y satisfy y = mx). Indeed the first possibility may **only** occur for **both** B and D **at the same time**, and is equivalent to $\mathbf{d_1 = d_2\sqrt{m^2+1}}$; and the second possibility may **only** occur for **both** B and D **at the same time**, and is equivalent to $\mathbf{d_2 = d_1\sqrt{m^2+1}}$. (The roles of B, D and A, C are **switched** when we select − instead of **+** in the above derived formula for k, with the formulas for **L** and **L' swapped**.) Observe that we may in fact set **m = tanγ**, where $γ = \phi/2$ is the **acute** angle

between the two glide reflection axes; with $m^2+1 = \tan^2\gamma+1 = \dfrac{1}{\cos^2\gamma}$, our condition becomes $|\mathbf{T_1}| = |\mathbf{T_2}| \times \cos\gamma$ **or** $|\mathbf{T_2}| = |\mathbf{T_1}| \times \cos\gamma$. [Notice that this condition is made all too obvious by figure 7.41, making all previous calculations above seem totally **redundant**; but our main goal was the determination of the composition center's **coordinates** in the **general case** (i.e., when the resulting rotation center lies on no glide reflection axis).]

In the case of the **p31m** pattern of figures 7.34 & 7.42, we may set, after rotating the coordinate system as above, $\mathbf{m = -\sqrt{3}}$; a bit of Geometry shows then that $|\mathbf{T_2}| = 2|\mathbf{T_1}|$, hence $d_2 = d_1\sqrt{m^2+1}$ and $|\mathbf{T_1}| = |\mathbf{T_2}| \times \cos\gamma$ are valid: **on-axis** rotations may therefore be seen as compositions of one genuine and one hidden glide reflection.

In the case of **perpendicular** glide reflections, $\lim\limits_{m\to\infty} \dfrac{\sqrt{m^2+1}}{m} = 1$ (the fraction approaching 1 as m approaches infinity) and $d_1/m = 0$ yield the centers $\mathbf{(\pm d_1, \pm d_2)}$, corroborating figure 6.54 and contributing to our understanding of **pgg** and **cmm** patterns. In the case of the latter, the off-axis centers are always produced by one reflection and one glide reflection perpendicular to each other; any pair of perpendicular glide reflections produces four centers lying, as we indicated in 6.9.3, on intersections of **reflection** axes, hence **not** on **glide** reflection axes.

In the case of the **p4g** pattern of figure 7.44 (and 4.55), working with the shown horizontal and diagonal glide reflection axes and vectors, observe that $m = \tan 45^0 = 1$, $d_1 = a/2$, and $d_2 = a/(2\sqrt{2}) =$ $d_1\cos 45^0$, so that $\dfrac{d_1+d_2\sqrt{m^2+1}}{m} = a$ and $\dfrac{d_1-d_2\sqrt{m^2+1}}{m} = 0$; here **a** stands for the length of the **horizontal** glide reflection vector (figure 7.44). The four intersection points (and fourfold centers) are (a/2, 0), (−a/2, 0), (a/2, −a), and (−a/2, a); the first two centers **do** indeed lie on the horizontal glide reflection axis:
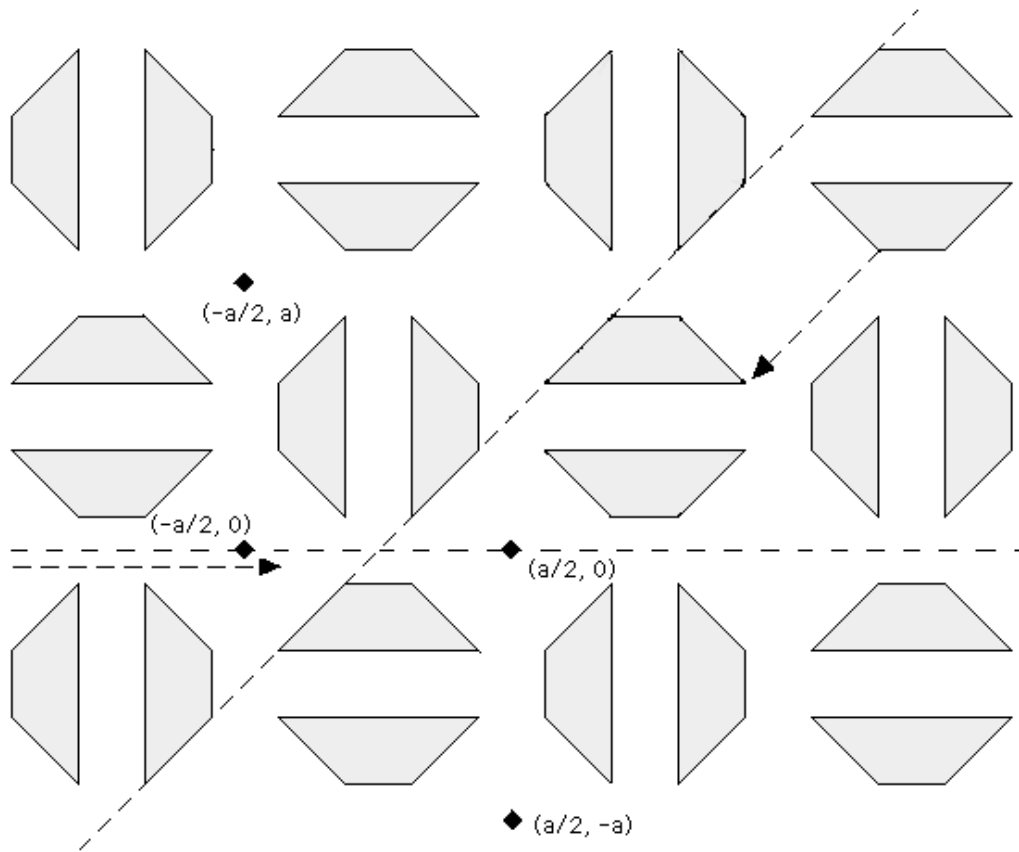
Fig. 7.44